11622–11642 *Nucleic Acids Research, 2017, Vol. 45, No. 20* *Published online 28 August 2017*
doi: 10.1093/nar/gkx746

Histone H1 depletion triggers an interferon response in cancer cells via activation of heterochromatic repeats

Andrea Izquierdo-Bouldstridge[1,†], Alberto Bustillos[1,†], Carles Bonet-Costa[1], Patricia Aribau-Miralbés[1], Daniel García-Gomis[1], Marc Dabad[2,3], Anna Esteve-Codina[2,3], Laura Pascual-Reguant[4], Sandra Peiró[4], Manel Esteller[5,6,7], Matthew Murtha[5], Lluís Millán-Ariño[1] and Albert Jordan[1,*]

[1]Institut de Biologia Molecular de Barcelona (IBMB-CSIC), Barcelona, Catalonia 08028, Spain, [2]CNAG-CRG, Centre for Genomic Regulation (CRG), Barcelona Institute of Science and Technology (BIST), Barcelona, Catalonia 08028, Spain, [3]Universitat Pompeu Fabra (UPF), Barcelona, Catalonia 08003, Spain, [4]Vall d'Hebron Institute of Oncology, Barcelona, Catalonia 08035, Spain, [5]Cancer Epigenetics and Biology Program, Bellvitge Biomedical Research Institute (IDIBELL), L'Hospitalet, Barcelona, Catalonia 08028, Spain, [6]Physiological Sciences Department, School of Medicine and Health Sciences, University of Barcelona (UB), Catalonia 08028, Spain and [7]Institució Catalana de Recerca i Estudis Avançats (ICREA), Barcelona, Catalonia 08028, Spain

Received May 26, 2017; Revised August 10, 2017; Editorial Decision August 11, 2017; Accepted August 15, 2017

ABSTRACT

Histone H1 has seven variants in human somatic cells and contributes to chromatin compaction and transcriptional regulation. Knock-down (KD) of each H1 variant in breast cancer cells results in altered gene expression and proliferation differently in a variant specific manner with H1.2 and H1.4 KDs being most deleterious. Here we show combined depletion of H1.2 and H1.4 has a strong deleterious effect resulting in a strong interferon (IFN) response, as evidenced by an up-regulation of many IFN-stimulated genes (ISGs) not seen in individual nor in other combinations of H1 variant KDs. Although H1 participates to repress ISG promoters, IFN activation upon H1.2 and H1.4 KD is mainly generated through the activation of the IFN response by cytosolic nucleic acid receptors and IFN synthesis, and without changes in histone modifications at induced ISG promoters. H1.2 and H1.4 co-KD also promotes the appearance of accessibility sites genome wide and, particularly, at satellites and other repeats. The IFN response may be triggered by the expression of noncoding RNA generated from heterochromatic repeats or endogenous retroviruses upon H1 KD. In conclusion, redundant H1-mediated silencing of heterochromatin is important to maintain cell homeostasis and to avoid an unspecific IFN response.

INTRODUCTION

There are five major classes of histones that participate in the correct folding of eukaryotic DNA into chromatin: the four core histones H2A, H2B, H3 and H4 which form an octamer that constitutes the nucleosome core particle, and the linker histone H1, which binds nucleosomes near the entry/exit sites of linker DNA. Stabilization of the condensed states of chromatin is the function most commonly attributed to linker histone (1), in addition to its inhibitory effect *in vitro* on nucleosome mobility (2) and transcription (3). Unlike core histones, the H1 histone family is more evolutionary diverse and many organisms have multiple variants or subtypes. In humans, histone H1 is a family of closely related single-gene encoded proteins, including seven somatic subtypes (from H1.1 to H1.5, H1.0 and H1X), three testis-specific variants (H1t, H1T2 and HILS1) and one restricted to oocytes (H1oo) (4–6). Among the somatic histone H1 variants, H1.1 to H1.5 are expressed in a replication-dependent manner, while H1.0 and H1X are replication-independent. H1.2 to H1.5 and H1X are ubiquitously expressed, H1.1 is restricted to certain tissues, and H1.0 accumulates in terminally differentiated cells.

One of the major open questions in the field is whether different somatic H1 subtypes are mainly redundant or have specific functions, functions that are perhaps cell type

*To whom correspondence should be addressed. Tel: +34 402 0487; Fax: +34 403 4979; Email: ajvbmc@ibmb.csic.es
†These two authors contributed equally to this work as first authors.
Present address: Lluís Millán-Ariño, Integrated Cardio Metabolic Centre, Department of Medicine Huddinge, Karolinska Institutet, Stockholm, Sweden.

specific. It is well established that H1 subtype composition varies through development and differentiation as well as between cell types and during disease associated processes such as neoplastic transformation (7–15). H1 subtypes are post-translationally modified, both at conserved and unique residues, and these modifications may modulate their interaction with an increasing number of proteins at the nucleoplasm or in chromatin (16,17). These interactions could explain some reported specific functions for certain H1 variants (18–23). Furthermore, genomic distribution of H1 variants is not absolutely redundant, with enrichment of different variants at certain chromatin types (reviewed in (6)). We have previously investigated the distribution of four H1 variants genome-wide in breast cancer cells, concluding that H1 variants are not distributed uniformly along the genome, H1.2 being the one showing the most specific pattern and strongest correlation with low gene expression (24,25).

Previous studies on the effect of H1 depletion on global gene expression have found no effect on the vast majority of genes, but rather have detected variant specific up- or down-regulation of small subsets of genes (26–29). However, it is not clear whether these effects are driven by variant specific roles to regulate particular promoters or play distinct roles depending on the cell type. For example, H1.2 has been reported to act as a coactivator by bridging between RNA polymerase II and components of the elongation apparatus in 293T cells, and to act as a corepressor by establishing a positive feedback loop with EZH2-mediated H3K27me3 deposition in MCF7 cells (30,31). Other H1 variants have been involved in chromatin compaction or gene silencing, such as H1.4 (21,22,32,33). In general, silent genes contain histone H1 at the promoter, and a 'H1 valley' appears upstream of transcription start site (TSS) upon gene activation (25,34,35).

Altering the expression of H1 variants has been proven useful to study the contribution of individual variants to nuclear processes and to investigate the effects of global H1 decrease. In mice, single or double H1 variant knock-outs have no apparent phenotype due to compensatory up-regulation of other subtypes (36). These reports have favored the view that H1 variants are redundant. Knocking-out additional subtypes cannot be fully compensated by up-regulation of the remaining subtypes, resulting in embryonic lethality and demonstrating that the total amount of H1 is crucial for proper embryonic development (37). Despite embryonic lethality, triple knock-out H1.2–H1.3–H1.4 (TKO) mouse embryonic stem (ES) cells were obtained with a 50% global reduction in total H1 (27). Among the observed effects of TKO, a subset of imprinted genes are up-regulated that correspond to specific CpG regions becoming demethylated. Yang *et al.* demonstrated that some H1 subtypes specifically interact with the DNA methyltransferases DNMT1 and DNMT3B to promote methylation of imprinted genes (38). Major satellite repeats are also de-repressed in TKO (39). More recently, changes in the epigenetic signature of thousands of potential regulatory sites across the genome of TKO ES cells have been described, clustered to gene-dense topologically associating domains (TADs) (40).

We have previously reported that depletion of single H1 subtypes by inducible RNA interference in cancer cells produced a range of phenotypic effects, suggesting non-redundant functions for some of the histone H1 variants in somatic cells (26). Here, we further investigate consequences of depleting H1 variants by simultaneous depletion of several variants in breast cancer cells. We generate two new short-hairpin-RNAs (shRNAs), one for the specific depletion of H1.4, and the other affecting the expression of several H1 genes (multiH1sh), but mainly H1.2 and H1.4 at the protein level. While H1.2 and H1.4 single knock-downs (KDs) decrease proliferation similarly, multiple H1 KD has drastic consequences on cell growth and induces a strong transcriptional interferon (IFN) response. We observed the activation of IFN signaling transducers, participation of cytosolic nucleic acids receptors, IFN synthesis and up-regulation of IFN-stimulated genes (ISGs). In parallel, satellites and endogenous retroviruses are also up-regulated and cytosolic RNA is increased. This is the first report of multiple H1 depletion in human cancer cells, and we show the importance of histone H1 to maintain heterochromatin integrity and to avoid a growth-inhibiting IFN response. We also show that pancreatic carcinomas characterized by a constitutively induced IFN response express low levels of several H1 variants.

MATERIALS AND METHODS

Cell lines, culturing conditions and treatments

Breast cancer T47D-MTVL cells (carrying one stably integrated copy of luciferase reporter gene driven by the MMTV promoter) or derivative cells, were grown at 37°C with 5% CO_2 in RPMI 1640 medium, supplemented with 10% FBS, 2 mM L-glutamine, 100 U/ml penicillin, and 100 μg/ml streptomycin, as described previously (26). HeLa cell line was grown at 37°C with 5% CO_2 in DMEM GlutaMax medium containing 10% FBS and 1% penicillin/streptomycin. MCF7 cell line was grown at 37°C with 5% CO_2 in MEM medium containing 10% FBS, 1% penicillin/streptomycin, 1% non-essential amino acids, 1% sodium pyruvate and 1% glutamine. Doxycycline (Sigma) was added at 2.5 μg/ml. IFNß (Sigma), Ruxolitinib (Selleckchem), BX795 (Selleckchem) and 2-aminopurine (Sigma) were added at indicated concentrations.

Drug-inducible and constitutive RNA interference

Inducible H1 knock-down cell lines were established from T47D-MTVL cells as described previously (26). Plasmids for the lentivirus vector-mediated drug-inducible RNA interference system (pLVTHM, ptTR-KRAB-Red, pCMC-R8.91 and pVSVG) were provided by Didier Trono (University of Geneva) (41). The 71-mer oligonucleotides for shRNA cloning into Mlu/ClaI-digested pLVTHM were designed, annealed and phosphorylated as recommended by Didier Trono (http://tronolab.epfl.ch/). Target sequences are GTCCGAGCTCATTACTAAA for H1–4sh and GA ACAACAGCCGCATCAAG for multiH1sh. For the production of viral particles containing the lentiviral vector and infections, see Sancho *et al.* (26). The inducible knocked-down cell lines were sorted in a FACSCalibur machine (Becton Dickinson) for RedFP-positive and GFP-positive fluorescence after 3 days of doxycycline (Dox) treat-

ment. For the constitutive depletion of TLR3, STING, MAVS, MDA5 and IFNAR, shRNA-expressing pLKO.1 vectors from the MISSION library (Sigma-Aldrich) were used. Viral particles production and infections were performed as described (26). Cells infected with the shRNA-expressing lentivirus were selected with 2 mg/ml puromycin (Sigma-Aldrich) 24 h after infection.

Stable expression of HA-tagged H1 variants

Generation of T47D derivative cells stably expressing HA-tagged H1 variants using the lentiviral expression vector pEV833.GFP provided by Eric Verdin (Gladstone Institutes) was achieved as described previously (26).

RNA extraction and reverse transcriptase (RT)-qPCR

Total RNA was extracted using the High Pure RNA Isolation Kit (Roche). Then, cDNA was generated from 100 ng of RNA using the Superscript First Strand Synthesis System (Invitrogen). Gene products were analyzed by qPCR, using SYBR Green Master Mix (Invitrogen) and specific oligonucleotides in a Roche 480 Light Cycler machine. Each value was corrected by human GAPDH and represented as relative units. Each experiment was performed in duplicate. Specific qPCR oligonucleotide sequences are available as Supplementary Table S1.

Histone and total protein extraction, gel electrophoresis and immunoblotting

Histone H1 was purified by lysis with 5% perchloric acid for 1 h at 4°C. Soluble acid proteins were precipitated with 30% trichloroacetic acid overnight at 4°C, washed twice with 0.5 ml of acetone and reconstituted in water. For isolation of total histones, cell pellets were resuspended in 1 ml of hypotonic solution [10 mM Tris–HCl (pH 8.0), 1 mM KCl, 1.5 mM $MgCl_2$, 1 mM PMSF, 1 mM DTT] and incubated on ice for 30 min. The nuclei were pelleted at 10 000 × g for 10 min at 4°C. Sulfuric acid (0.2 M) was added to the pellet to extract the histones on ice for 30 min. The solution was centrifuged at 16 000 × g for 10 min at 4°C. TCA was added to the supernatant in order to precipitate histones and the precipitate was washed with acetone and finally resuspended in water. For isolation of total protein, cells were resuspended with Lysis Buffer [25 mM Tris-H–Cl (pH 7.5), 1% SDS, 1 mM EDTA (pH 8), 1 mM EGTA (pH 8), 20 mM B-glycerolphosphate] containing protease and phosphatase inhibitors, and boiled 20 min at 95°C. Cell lysates were obtained by centrifugation and protein concentration was determined by Micro BCA protein assay (Pierce). Purified histones or cell lysates were exposed to SDS-PAGE (12%), transferred to a PVDF membrane, blocked with Odyssey blocking buffer (LI-COR Biosciences) for 1 h, and incubated with primary antibodies overnight at 4°C and with secondary antibodies conjugated to fluorescence (IRDye 680 goat anti-rabbit IgG, Li-Cor) for 1 h at room temperature. Bands were visualized in an Odyssey Infrared Imaging System (Li-Cor). Polyclonal antibodies specifically recognizing human H1 variants, including those generated in our laboratory (26), are available from Abcam: H1.0 (ab11079), H1.2 (ab17677), H1.3 (ab24174), H1-T146p (ab3596), H1.5 (ab24175) and antiH1X (ab31972). Other antibodies used were: H1 AE-4 (Millipore, 05-457), beta-tubulin (Sigma, no. T4026), H3K4me3 (Abcam, ab8580), H3K9me3 (Abcam, ab8898), H3K27me3 (Millipore, 07-449), H4K20me3 (Abcam, ab9053), HP1α (Active Motif, 39295). H1-T146p was used to identify H1.4 by immunoblot, as the immunogen was a synthetic peptide derived from within residues 100–200 of human H1.4, phosphorylated at T146; this antibody could also recognize phospho T146 in H1.2, H1.3 (both 88% sequence identity with immunogen). To our knowledge this is the best available antibody to detect loss of H1.4 despite targeting a uniquely phosphorylated residue. To quantify H1 depletion with Coomassie staining, we load different amounts of total histones and choose the ones that showed the best linear range. After scanning with Image Gauge, individual histone H1 and H4 bands were quantified and H1 was expressed relative to H4, and relative to untreated cells. These were approximate quantifications due to the limitations of Coomassie staining of histone preps.

Immunofluorescence

One milliliter of hypotonic MAC buffer [50 mM glycerol, 5 mM KCl, 10 mM NaCl, 0.8 mM $CaCl_2$ and 10 mM sucrose] was added to 0.5 million cells (resuspended in 1 ml RPMI 1640 medium) and incubated at room temperature for 5 min. 400 μl were spun down for 10 min at 500 rpm in a TermoShandon Cytospin 4 using a single-chamber Cytospin funnel as described in (42). Cells were air-dried for 1h at room tempearature. Then, fixed with 4% paraformaldehyde for 1h at room temperature. After three washes, they were permeabilized with 0.2% Triton X-100 for 15 min at room temperature and blocked with 3% bovine serum albumin for 1 h at room temperature. Then, the cells were incubated with primary antibody recognizing dsRNA (Scicons J2, English and Scientific Consulting Kft, Hungry) diluted in the blocking buffer, over-night at 4°C. After the pertinent washes, the secondary antibody Alexa Fluor 488 donkey anti-mouse (Life Technologies, A21202) was added for 1 h at room temperature in darkness. Nuclei were stained with DAPI, coverslips mounted using Mowiol, and samples were visualized by confocal laser scanning microscopy using a Leica TCS SP5 system.

Cell proliferation analysis

Cells of interest expressing an shRNA (GFP-positive) were mixed 1:1 with parental cells (GFP-negative) and cultured. Every three days, the cells were split and the percentage of cells that were GFP-positive was measured by FACS.

MNase digestion

Cells treated or not with Dox for six days were collected, resuspended and incubated for 10 min at 4°C in Buffer A [10 mM Tris–HCl pH7.4, 10 mM NaCl, 3 mM $MgCl_2$, 0.3 M Sacarosa and 0.2 mM PMSF], after that 0.2% of NP40 was added and incubated 10 min more at 4°C. After centrifugation, pellets were resuspended in Buffer A + 10 mM $CaCl_2$ and 0.4 u of MNase per 5 millions of nuclei and incubated

at 37°C. At different incubation times, MNase reaction was stopped by adding 10 mM EDTA pH 8. DNA was purified using EZNA Tissue DNA columns (OMEGA VWR) and run on a 2% agarose gel.

Chromatin immunoprecipitation (ChIP)

Immunoprecipitation of chromatin was performed according to the Upstate (Millipore) standard protocol. Briefly, cells were fixed using 1% formaldehyde for 10 min at 37°C, harvested and sonicated to generate chromatin fragments of 200–500 bp. Then, 30 μg of sheared chromatin was immunoprecipitated overnight with 2 μg of antibody. Immunocomplexes were recovered using 20 μl of protein A magnetic beads, washed and eluted. Cross-linking was reversed at 65°C overnight and immunoprecipitated DNA was recovered using the PCR Purification Kit from Qiagen. Genomic regions of interest were identified by real-time PCR (qPCR) using SYBR Green Master Mix (Invitrogen) and specific oligonucleotides in a Roche 480 Light Cycler machine. Each value was corrected by the corresponding input chromatin sample. Oligonucleotide sequences used for the amplifications are available on request.

mRNA library preparation and sequencing (RNAseq)

The library from total RNA was prepared using the TruSeq®Stranded Total Sample Preparation kit (Illumina Inc.) according to manufacturer's protocol. Briefly, rRNA was depleted from 0.5 ug of total RNA using the Ribo-Zero Gold Kit followed by fragmentation by divalent cations at elevated temperature resulting into fragments of 80–450nt, with the major peak at 160nt. First strand cDNA synthesis by random hexamers and reverse transcriptase was followed by the second strand cDNA synthesis, performed in the presence of dUTP instead of dTTP. Blunt-ended double stranded cDNA was 3′adenylated and the 3′-'T' nucleotide at the Illumina indexed adapters was used for the adapter ligation. The ligation product was amplified with 15 cycles of PCR. Each library was sequenced using TruSeq SBS Kit v3-HS, in paired end mode with the read length 2 × 76 bp. We generated minimally 37 million paired end reads for each sample run in a fraction of a sequencing lane on HiSeq2000 (Illumina, Inc) following the manufacturer's protocol. Images analysis, base calling and quality scoring of the run were processed using the manufacturer's software Real Time Analysis (RTA 1.13.48) and followed by generation of FASTQ sequence files by CASAVA.

RNAseq data analysis

The mapping of the reads against the human reference genome (GRCh38) was done using the STAR program (version 2.5.1b) (43) and the quantification of genes was done with the RSEM program (version 1.2.28) (44). Differential expression analysis was done with DESeq2 (version 1.10.1) (45). Heatmaps, correlation scatter plot and boxplots were done using in-house R scripts. The expression values are those generated by DESeq2 using variance stabilizaing transformations. Genes differentially expressed by IFN treatment were selected from Interferome database (version 2.01) (46) applying a filter of 2 < fold-change < –2 and those differentially expressed in more than one experiment. Enrichment of transcription factor binding DNA motifs was done using Homer software (47). Gene ontology enrichment analysis was performed using the R package 'goseq' (version 1.18.0) (48) and reduced by semantic similarity using REViGO software (49). Pathway enrichment analysis and figures were generated using ReactomeFIPlugin (50) for Cytoscape (51). To perform the enrichment analysis of repetitive sequences the RNA-seq reads were mapped to the Repbase database (version 21.02) (52) using Bowtie aligner (default parameters) (53). We only considered those reads which both paired-end reads were aligned to the same repetitive sequence. To test for significance a Fisher exact test was performed. Significantly enriched repetitive sequence were those with a adjusted *P*-value < 0,05 and not enriched in RDsh samples.

Assay for transposase-accessible chromatin with high-throughput sequencing (ATAC-seq)

ATAC experiment was performed as described (54). 75 000 cells treated were harvested and treated with transposase Tn5 (Nextera DNA Library Preparation Kit, Illumina). DNA was purified using MinElute PCR Purification Kit (Qiagen). All samples were then amplified by PCR using NEBNextHigh-Fidelity 2× PCR Master Mix (New Englands Labs.) and primers containing a barcode to generate the libraries. DNA was again purified using MinElute PCR Purification Kit and samples were sequenced using Illumina HiSeq 2500 system. Paired-end reads were first trimmed to 30 bp to remove adapter sequences. Then, aligned to the reference genome (hg19) using bowtie software (53). Duplicated reads and those mapping to the mitochondrial chromosome were removed. Accessibility peaks were obtained using MACS2 peak caller software (55). Average accessibility profile around the TSS of selected genes and pie charts representing the annotation of peaks was performed using CEAS software (56). For the repeats accessibility analysis, annotated repeats were taken from the RepeatMasker track from the UCSC and the number of peaks overlapping them computed. For the analysis of peaks overlapping up- or down-regulated genes at the coding regions or promoter, or repeats, a permutation test (10^4 permutations) was performed using the R package regioneR (57).

Expression data accession numbers

RNAseq data is available in the Gene Expression Omnibus (GEO) database under the accession number GSE83277. Microarray data accession numbers are GSE11294 and GSE12299. ATACseq data accession number is GSE100762.

Human H1 variant nomenclature

The correspondence of the nomenclature of the human H1 variants with their gene names is as follows: H1.0, H1F0; H1.1, HIST1H1A; H1.2, HIST1H1C; H1.3, HIST1H1D; H1.4, HIST1H1E; H1.5, HIST1H1B; and H1X, H1FX.

RESULTS

Simultaneous depletion of multiple H1 variants in breast cancer cells impairs cell growth drastically

We have previously reported the effects of the inducible depletion of six somatic histone H1 variants on cell growth and gene expression in breast cancer cells (24,26). H1.2 depletion caused cell-cycle arrest in G1 phase, while H1.4 KD caused cell death in T47D cells. Each variant KD altered the expression of small distinct subsets of genes.

We have designed and assayed new shRNAs targeting H1. One of such shRNAs (sh120; H1.4sh) was specific for H1.4 (Figure 1A and B), while another (sh225; multiH1 or mH1sh from now on) reduced the expression of several H1 transcripts, although only H1.2 and H1.4 proteins were seen depleted consistently when tested by immunoblotting after 6 days of Doxycycline induced shRNA expression (Figure 1A and C, and Supplementary Figure S1). H1.3 was also seen partially depleted in some experiments. The two new shRNAs caused H1.0 up-regulation, both at the mRNA and protein level. This was previously observed for H1.2 KD, but not for the other H1 variants (26). Coomassie staining of histones extracted from multiH1 KD cells showed that the total content of H1 was reduced to ca. 70% despite of H1.0 up-regulation (Figure 1C and D). The intensity of protein bands containing H1.2 and H1.4 were decreased.

In addition, multiH1sh expression caused a significant reduction in global nucleosome spacing as assessed by Micrococcal nuclease digestion of bulk chromatin (Figure 1E and Supplementary Figure S2). This was almost undetectable upon H1.4 KD, but was previously described for H1.2 depletion in breast cancer cells (26).

Expression of both shRNAs impaired cell proliferation (Figure 1F). The effect of inhibiting simultaneously H1.2 and H1.4 in multiH1 KD cells on the growth rate was additive compared to single H1 depletion. H1 depletion increased the number of cells in G1 phase of the cell cycle and reduced cells in S phase, with the effects of multiH1sh being more pronounced than H1.4sh (data not shown).

Transcriptome changes upon histone H1 variants knock-down

We studied the consequences on global gene expression of multiple H1 KD and H1.4-specific depletion compared to the random shRNA using RNAseq. Data confirmed the efficacy of H1.4 and multiH1 shRNAs to inhibit the corresponding H1 genes without significant compensations other than some H1.0 up-regulation (Figure 2A). Results were compared with microarray data obtained before with the KD of the other variants (24,26). As previously described, depletion of individual H1 variants altered the expression of small subsets of genes, considerably specific for each variant, and containing both up- and down-regulated genes in different proportions. The inhibition of multiple H1s affected a larger number of genes, some already observed in single variant KDs (Figure 2B and Supplementary Table S2). In particular, 38% of genes affected in H1.4sh were also affected in multiH1sh (which also targets H1.4), while only 20–28% of the genes affected in the other single variant KDs (H1.0, H1.2, H1.3 or H1.5) were significantly affected in the multiH1 KD.

Among genes up-regulated in the multiH1 KD, there were many interferon-stimulated genes (ISGs) (Figure 2C). Comparison of our data with the Interferome database containing microarray data of IFN-treated cells, showed that 36% of the up-regulated and 18% of the down-regulated genes in the multiH1 KD were known to also respond to short- or long-term INF treatments. This is in comparison to the 6% of the total transcriptome known to be susceptible to IFN treatment (Figure 2C). Almost all the multiH1 KD up-regulated genes with the highest fold-change are ISGs. Moreover, fold-change gene induction upon multiH1 depletion was proportional (positive correlation) to the fold-change induction in response to IFN in multiple experiments deposited in the Interferome database (Figure 2D).

Motif analysis in the promoters of multiH1sh deregulated genes found significant enrichment of interferon-stimulated response elements (ISRE), binding sites for interferon-responsive transcription factors (IRFs), but not in gamma-activated sites (GAS) (Figure 2E). ISRE are found in type I IFN-responsive genes, while GAS elements are present in type II IFN-stimulated genes. Down-regulated genes contained motifs for E2F, Sp1 and NFY transcription factors (q-value$<$0.0001). Gene-ontology analysis confirmed the enrichment of IFN signaling pathways in the multiH1sh up-regulated genes, while multiH1sh and single H1.4sh down-regulated genes showed GO-terms related to cell-cycle regulation (Figure 2F). No significantly enriched DNA motifs were found in the promoters of H1.4sh affected genes, and no GO-terms were found for the H1.4sh up-regulated genes.

Interestingly, basal gene expression (without doxycycline) of genes up-regulated in H1 KD cells was significantly lower than basal expression of genes down-regulated, despite of the variability within each gene set (Figure 2G). After H1 depletion, overall gene expression of up- and down-regulated genes was more similar. This observation could suggest that histone H1 may play a role in the maintenance of repression in the up-regulated genes. Nevertheless, both up- and down-regulated genes showed an average gene expression above the average of RefSeq genes or even above the expressed transcriptome (Supplementary Figure S7A).

In conclusion, depletion of individual H1 variants effects a small subset of genes, while multiple variant knock-down alters gene expression extensively, larger than the additive effect of individual variants, including an unexpected large proportion of type I interferon-stimulated genes. The fact that there is limited overlap between deregulated genes in H1.2 or H1.4 KDs and multiH1 KD suggests that these genes are not directly regulated by these variants, but the combined depletion of the two variants may trigger an interferon response.

Induction of interferon-stimulated genes upon combined depletion of histone H1 variants

We next sought to understand how the interferon response is induced in H1-depleted breast cancer cells. Either H1 is particularly involved in repressing the promoters of ISGs with little variant specificity, or general H1 depletion from

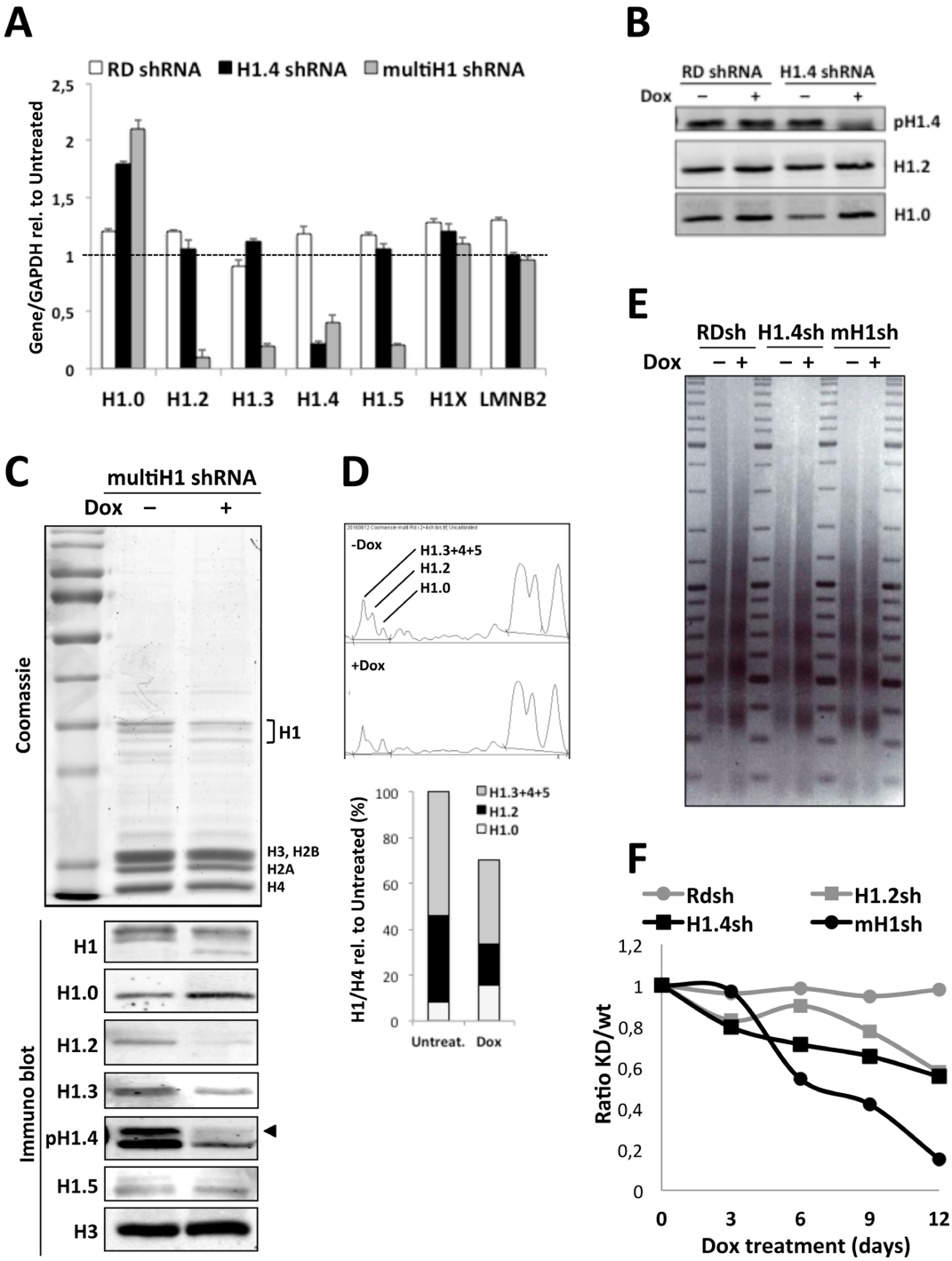

Figure 1. Inducible shRNAs for the depletion of histone H1 variants in human breast cancer cells. (**A**) Expression of H1 variants upon inducible expression of new shRNAs. T47D derivative cells stably infected with inducible lentiviruses for the expression of random, H1.4 or multi-H1 shRNAs were treated or not for 6 days with doxycycline (Dox), RNA was extracted and gene expression was analyzed by RT-qPCR with oligonucleotides for the indicated H1 genes. Gene expression in response to Dox is expressed corrected by GAPDH and relative to untreated cells. Values represent the mean and SD of a representative experiment performed in triplicate. (B and C) H1 depletion was additionally tested by immunoblotting with the H1 variant-specific antibodies indicated. H1 phospho-T146 antibody was used to detect H1.4 (pH1.4) (see Materials and methods). (**B**) H1 from random and H1.4 shRNA cells treated or not with Dox for 6 days were acid-extracted. (**C**) Total histones were extracted from multi-H1 shRNAs cells, run on SDS-PAGE and stained with Coomassie or immunoblotted. (**D**) Coomassie-stained histone bands were scanned and quantified. The graph denotes the decrease of total H1 and variations of each H1-containing band (corrected to histone H4) upon Dox treatment of multiH1 KD cells. (**E**) H1 KD causes a reduction in nucleosome spacing. Nuclei from the KD cells indicated treated or not with Dox for 6 days were treated with MNase and the profile of bulk chromatin was analyzed in gel electrophoresis. A representative experiment is shown. (**F**) Effect of H1 depletion on cell proliferation. In order to measure the effect of H1 depletion on cell proliferation, each of the H1 variant KD cell lines indicated (RFP and GFP-positive) was mixed 1:1 with parental T47D cells (RFP and GFP-negative) and treated with Dox. Every three days, cells were split and the percentage of double-positive cells was measured by FACS. Data is expressed as ratio of positive (KD) versus negative (wild-type) cells along time and corresponds to a representative experiment performed in duplicate.

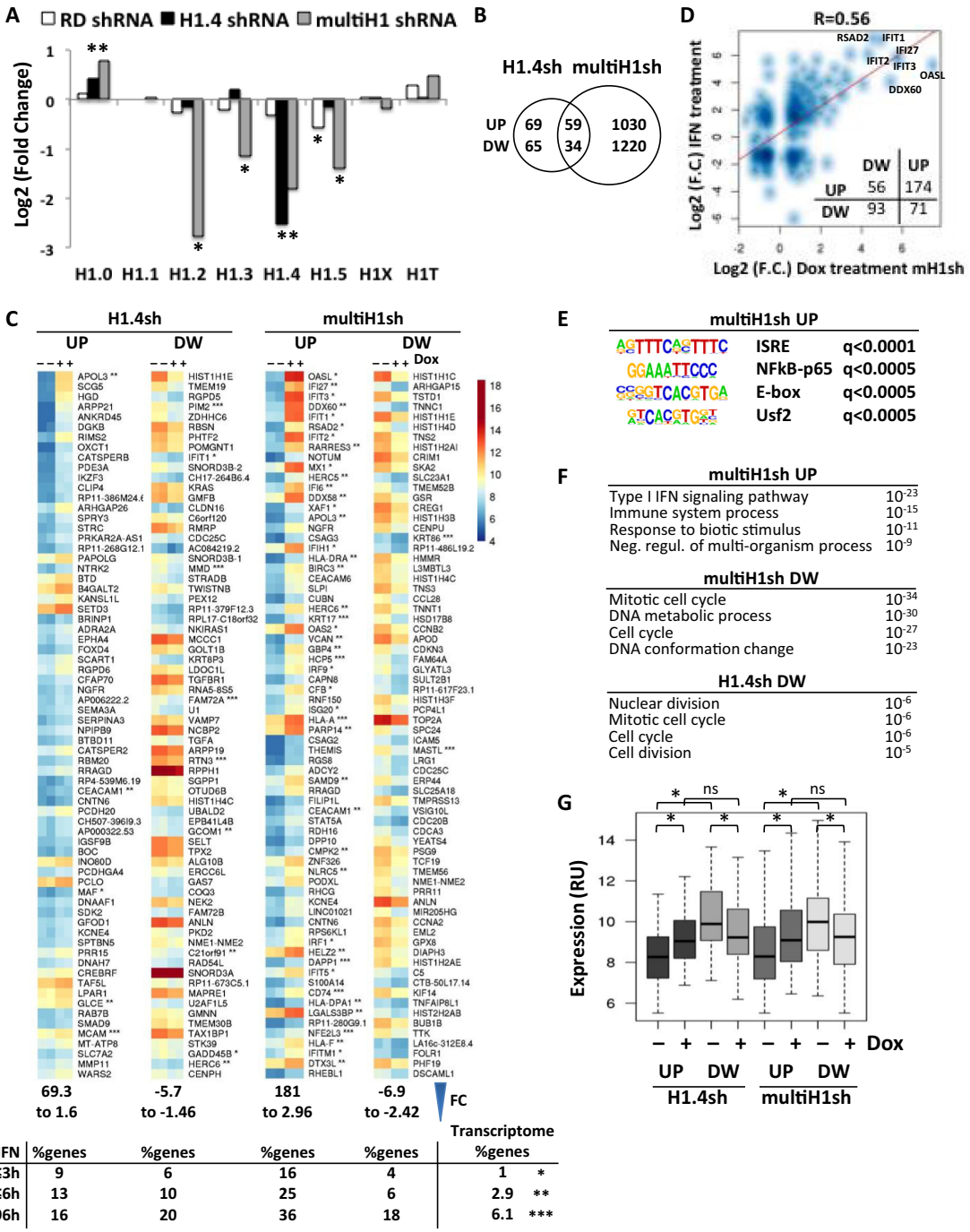

IFN	%genes	%genes	%genes	%genes	%genes	Transcriptome
≤3h	9	6	16	4	1	*
≤6h	13	10	25	6	2.9	**
≤96h	16	20	36	18	6.1	***

Figure 2. Transcriptome changes upon histone H1 variants knock-down. (**A**) H1 variants expression in the random, H1.4 and multiH1 KD cells upon a 6-day Dox treatment extracted from RNAseq data. Data is shown as Log2 of the fold-change Dox-treated compared to untreated. Significant changes with *P*-value < 0.001 are shown with asterisks. (**B**) Venn diagram showing the number of genes up- or down-regulated in H1.4 and multiH1 KD cells (and not changing in random shRNA ±Dox samples) established by RNAseq (FC ≥ 1.4, adjusted *P*-value ≤ 0.05). (**C**) Genes most highly up- (UP) and down-regulated (DW) in H1.4 and multiH1 KD cells (70 genes of each are shown), not changing in RDsh samples, ordered according to fold-change from top to down. Genes that respond to IFN according to the Interferome data base (in more than one experiment, with FC ≥ 2) are labeled with asterisks: *, 0.5–3 h IFN-treatment; **, 3–6 h IFN; ***, 6–96h IFN. The table below shows the percentage of genes up- or down-regulated in each H1 KD (FC ≥ 1.4, adjusted *P*-value ≤ 0.05), or in the total transcriptome, that respond to IFN. (**D**) Correlation scatter plot between gene expression fold-change in multiH1sh cells upon Dox-treatment (RNAseq data, FC ≥ 1.4) and fold change upon IFN treatment (Interferome data base, FC ≥ 2). R is the Pearson's correlation coefficient, with *P*-value < 0.0001. Insert table: Number of genes deregulated in multiH1sh that are up- or down-regulated in response to IFN. (**E**) Enriched transcription factor binding DNA motifs in multiH1sh up-regulated genes. (**F**) Analysis of enriched gene-ontology terms in H1 KD deregulated genes. GO terms (biological processes) were collapsed by semantic similarity using REVIGO software and the four more significant terms are shown. Enrichment score is shown as adjusted *P*-value. (**G**) Box plots showing the expression profiles of genes up- and down-regulated in H1.4 and multiH1 KD cells, treated or not with Dox. Significance was tested using the Kolmogorov–Smirnov test (**P*-value < 0.05).

the genome somehow triggers the response by promoting IFN synthesis. First, we confirmed by reverse transcription and semi-quantitative PCR (RT-qPCR) the induction of several ISGs in multiH1sh but not control random shRNA (RDsh) cells upon 6-days of doxycycline treatment (Figure 3A). Some of the ISGs showed inductions as high as 100- to 300-fold. A 3-days time curve treatment with doxycycline showed that H1 transcripts, mainly H1.2 and H1.4, were significantly depleted after 12 h (Figure 3B). ISG up-regulation was first observed 48 h after treatment start and was increased at 72 h, both for genes highly induced (IFI27, IFIT2 and IFI6) or less induced (STAT1, IRF1 and IRF7). Interestingly, the gene encoding for IFN-ß (IFNB), which was not found up-regulated in the RNAseq data after 6 days treatment, was induced at early time points (Figure 3B). In a longer H1 KD time curve, ISG expression was progressively increased up to 9 or 12 days of doxycycline treatment (Figure 3C and Supplementary Figure S3). Instead, IFNB, after peaking at 3 days, decreased its expression, explaining why it was not detected in the RNAseq experiment (data not shown). In the same experiment, upon removal of doxycycline at day 3, recovery of H1 variants transcript accumulation was not observed at day 6 but it was at day 9. Upon H1 expression recovery, ISGs were efficiently down-regulated to basal level, indicating that the IFN response induction can be reversed upon H1 recovery.

Induction of ISGs was not observed in single H1 KDs, neither in genome-wide data (microarrays and RNAseq), nor by RT-qPCR. Figure 3D shows the absence of ISGs induction in H1.2 KD constructed in T47D, MCF7 and HeLa cell lines. In contrast, when the H1.2 inducible shRNA was introduced into T47D H1.4 KD cells, to obtain a new multiH1 KD cell line (H1.4/H1.2sh; 80–90% of total H1), ISGs were highly induced upon doxycycline treatment (Figure 3E and Supplementary Figure S4). This indicates that the combined depletion of H1.2 and H1.4 in T47D with variant-specific shRNAs is sufficient to promote the IFN response and validates results obtained with the multiH1sh construct. Induction of ISGs was not unique to T47D cells as it was also observed in MCF7 infected with the multiH1sh, where H1.2 and H1.4 are depleted (data not shown).

We also tested whether other H1 KD combinations were able to reproduce this effect. The H1.5 inducible shRNA was introduced into T47D H1.2 or H1.4 KD cells and all Dox-induced H1 depletions tested by RT-qPCR, Coomassie and immunoblot. Total H1 content was reduced to 60–80% of wild-type (Supplementary Figure S5). Simultaneous depletion of H1.2 and H1.5 caused ISG up-regulation to some extent (Figure 3F). Nonetheless, fold-change induction of ISGs was much higher in H1.4/H1.2sh than in H1.2/H1.5sh cells (Figure 3E versus F). No ISG up-regulation was observed upon combined depletion of H1.4 and H1.5, suggesting that H1.2 depletion is crucial, although not sufficient, to induce the IFN response. Interestingly, the total amount of histone H1 depleted in H1.4/H1.5sh or H1.2/H1.5sh cells was not lower than the achieved with the other KD combinations (multiH1sh or H1.4/H1.2sh), indicating that the induction of the IFN response is variant specific and not likely due to total H1 reduction. Finally, H1.4/H1.5sh and H1.2/H1.5sh cells were further infected with the H1.3 inducible shRNA. While ISGs remained unaltered in H1.4/H1.5/H1.3sh cells, they were further induced in H1.2/H1.5/H1.3sh cells, still to lesser levels than H1.4/H1.2sh (Supplementary Figure S5C).

To test whether ISGs induction in multiH1sh cells could be complemented by overexpressing distinct H1 variants, we infected multiH1sh cells with lentiviruses expressing GFP and hemaglutinin peptide (HA)-tagged H1.2, H1.3 or H1.4. Efficient infection was confirmed by FACS analysis of GFP (80–90% infection) as well as RT-qPCR of H1 expression (Figure 3F). Although the recombinant H1 genes were sensitive to the multiH1 shRNA and expression of HA-tagged H1s was diminished upon Dox treatment, some expression remained above the levels found in parental multiH1sh cells, sufficient to observe partial complementation of the effect of multiH1 KD on ISGs induction (Figure 3F). Immunoblotting confirmed that HA-tagged H1s were still present after Dox treatment (Supplementary Figure S6). It is noteworthy that not only H1.2 or H1.4 overexpression partially complemented the multiH1 KD, but also H1.3, indicating that the IFN response induction by H1 depletion is not fully variant-specific.

Synthesis of interferon and induction of IFN signaling upon multiple H1 depletion

Together these data suggest that H1 depletion mimics or induces the IFN response, for example inducing IFN production. The IFN response is triggered in cells when foreign DNA or RNAs are recognized by cytosolic nucleic acid sensors that trigger a signaling cascade, leading to the activation and nuclear entry of IFN-responsive transcription factors (IRFs). These IRFs then bind and regulate the promoter of IFN-encoding genes and other ISRE-containing target genes. IFN is secreted to the media, where it binds and activates IFN receptors at the surface of responsive cells, which activate the Janus kinase (JAK)-STAT signaling pathway leading to further activation of IRFs and ISRE-containing target genes (by type I IFNs), or to the activation of genes containing gamma-activated sites (GAS) elements (by type II IFN). IFN stimulation classically results in an anti-viral immune response and also has anti-tumor effects inducing ISGs with anti-proliferative and pro-apoptotic functions (58,59).

Induction of ISGs upon H1 depletion could be mediated by IFN synthesis, because, as reported above, the IFNB gene (but not IFNA) was up-regulated at short times after Dox addition to multiH1sh cells (Figure 3B). First, we confirmed that T47D derivative cells were sensitive to commercial IFN-ß, and induction of ISGs by IFN-ß at 0.15 μg/ml was comparable to the upregulation achieved by the combined KD of H1.4 and H1.2 (Figure 4A). ISG induction was not increased by higher concentrations of IFN-ß (1.2 μg/ml), but was synergistic with the effect of H1.4/H1.2 KD (Dox treatment), suggesting that ISG induction by H1 depletion is not only due to IFN synthesis. The effect of IFN-ß was not potentiated by knocking-down individually H1.2 or H1.4 (Figure 4A). We then tested whether IFN was being produced and liberated to the extracellular media. Conditioned growth media of multiH1 KD cells treated with Dox for 3 days was added to wild-

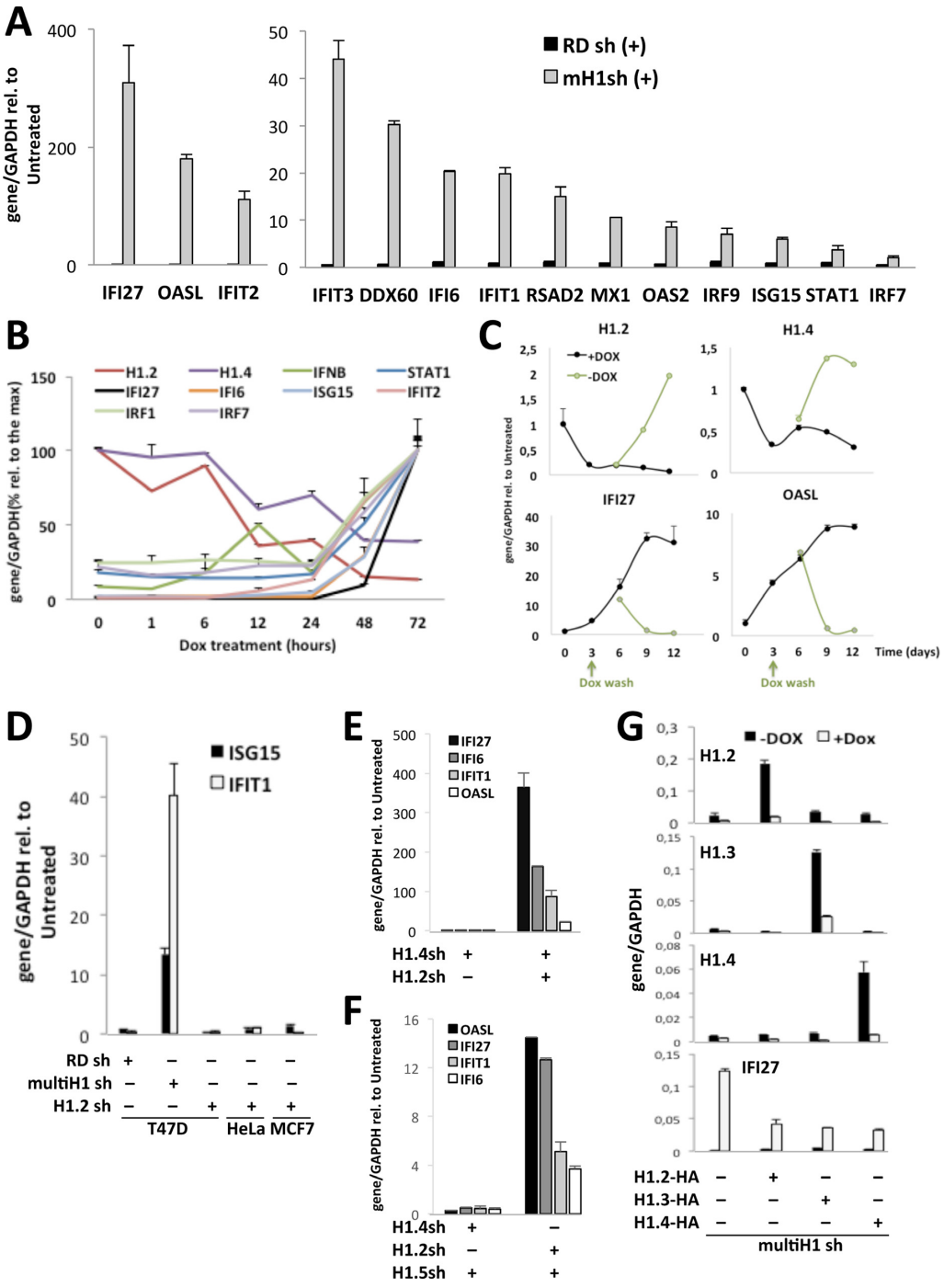

Figure 3. Induction of interferon-stimulated genes upon combined depletion of histone H1 variants. (**A**) Induction of ISGs in multiH1 KD cells. T47D cells containing RDsh or multiH1sh were treated or not with Dox for 6 days and gene expression was tested by RT-qPCR with oligonucleotides for the indicated genes. Gene expression in response to Dox is expressed corrected by GAPDH and relative to untreated cells. (**B**) ISG and H1 variants expression along time after Dox treatment. T47D cells containing multiH1sh were treated with Dox up to 72 h and gene expression was tested as in (A). Gene expression is corrected by GAPDH and relative to the highest data point for each gene. (**C**) H1 expression recovery and reversal of ISG expression after Dox removal. MultiH1 KD cells were treated with Dox for 3 days and split, washed and maintained without Dox or left with Dox up to 12 days. Gene expression was tested by RT-qPCR every 3 days, corrected by GAPDH and shown relative to untreated (time 0). (**D**) ISG induction occurs in multiH1sh but not H1.2sh cells. The indicated cell lines containing RDsh, multiH1sh or H1.2sh were treated or not with Dox for 6 days and ISG15 and IFIT1 gene expression was tested and expressed as in (A). (**E**) ISGs are induced in a double H1.4/H1.2 KD cell line. T47D cells containing H1.4sh were infected or not with the H1.2 shRNA-expressing lentivirus. Resulting cells were treated or not with Dox for 6 days and ISG expression was tested as in (A) and expressed relative to untreated cells. (**F**) ISG induction in a double H1.2/H1.5 KD cell line. T47D cells containing H1.2sh or H1.4sh were infected with an H1.5 shRNA-expressing lentivirus. Resulting cells were treated or not with Dox for 6 days and ISG expression was tested as in (A). (**G**) H1 overexpression in multiH1 KD cells partially blocks ISG up-regulation. T47D cells containing multiH1sh were infected or not with a lentivirus for the expression of HA-tagged H1.2, H1.3 or H1.4 variants. Resulting cells were treated or not with Dox for 6 days and H1 variant and ISG gene expression was tested as in (A). Values represent the mean and SD of representative experiments performed in triplicate.

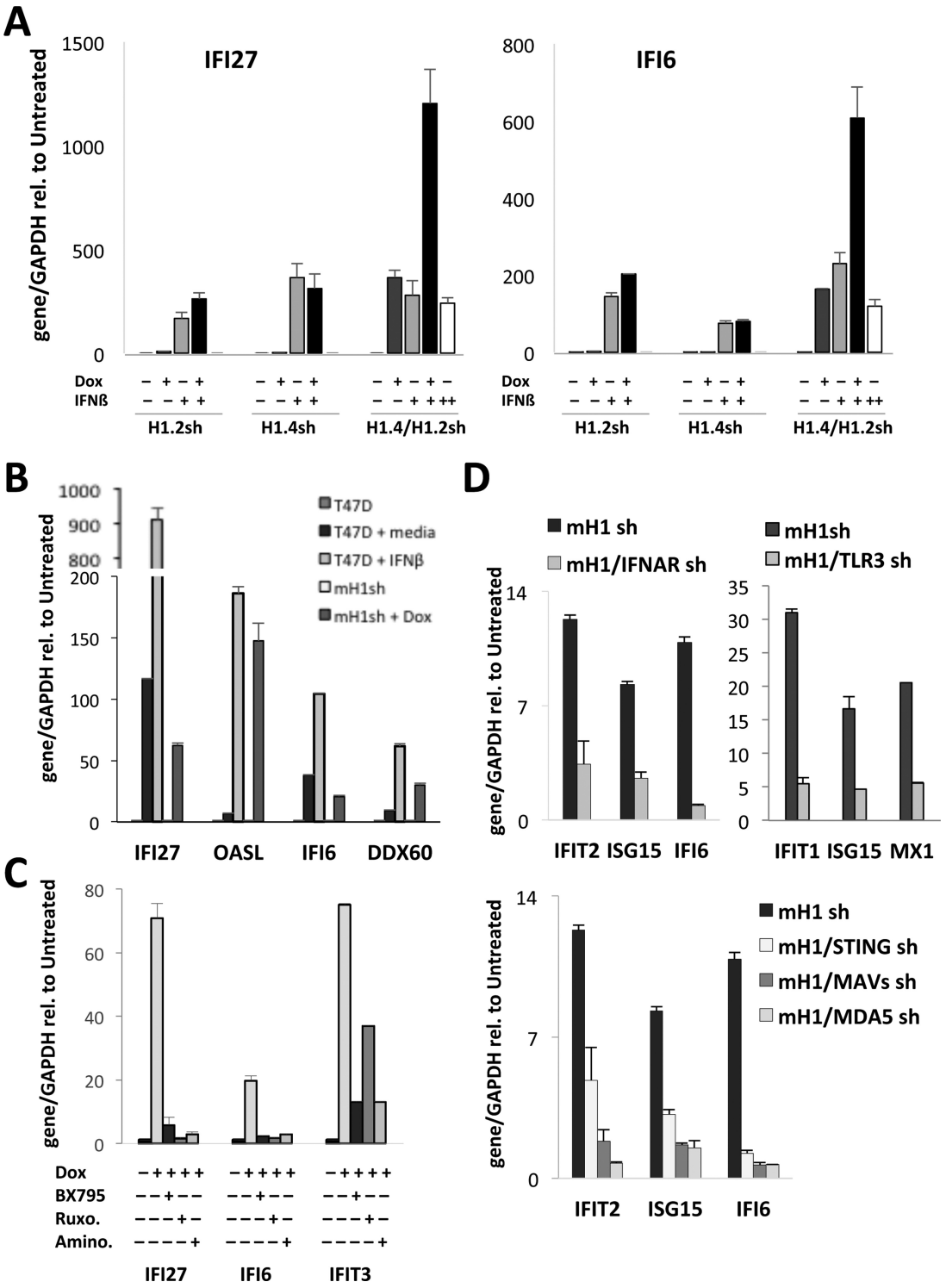

Figure 4. Activation of the interferon response pathway upon depletion of histone H1. (**A**) IFN-ß enhances ISG induction in H1.4/H1.2sh cells. T47D cells containing H1.2sh, H1.4sh or H1.4/H1.2sh were treated or not with Dox for 6 days and IFN-ß at 0,15 (+) or 1,2 (++) μg/ml was added for the last 8 h before analysis of ISG expression, corrected by GAPDH. (**B**) ISG induction by IFN liberated to the media. T47D cells containing multiH1sh were treated with Dox for 3 days, media was collected and added to wild-type T47D cells for 24 h. For comparison, T47D cells were treated with commercial IFN-ß (0.15 μg/ml) for 24 h, and multiH1sh cells treated with Dox for 3 days. ISG expression was tested by RT-qPCR, corrected by GAPDH and expressed relative to untreated cells. (**C**) ISG induction is blocked with IFN pathway inhibitors. T47D multiH1sh cells were treated or not with Dox, 0.5 μM BX795, 1 μM ruxolitinib or 10 mM 2-aminopurine, for 3 days, and ISG expression was tested as in (A). Gene expression is corrected by GAPDH and relative to the highest data point for each gene. (**D**) Blocking ISG induction by knocking-down type-I IFN receptor or IFN pathway sensors and transducers. T47D multiH1sh cells stably expressing shRNAs against IFNAR1, TLR3 (upper panels), STING, MAVS or MDA5 (lower panel) were treated or not with Dox for 6 days and ISG expression was tested as in (A) compared to parental multiH1sh cells. Gene expression is corrected by GAPDH and represented relative to untreated cells. Values represent the mean and SD of representative experiments performed in triplicate.

type T47D cells and ISG expression was tested. The media was able to stimulate expression of ISGs to some extent, although to a lesser extent than was achieved by treating cells with commercial IFN-ß (Figure 4B). Moreover, when a shRNA against the type I IFN receptor IFNAR1 was introduced into multiH1sh cells, ISG stimulation upon Dox treatment was partially affected (Figure 4D). In conclusion, multiH1 depletion has an effect on the induction of ISGs that is partially explained by the production and reentry of IFN.

To further determine the involvement of signaling associated to the IFN response, we analyzed the effect of inhibitors of kinase TBK-1, an intermediate in the sensing cascade, and Janus kinase (JAK) 1 and 2, BX795 and Ruxolitinib, respectively. Both inhibitors impaired the up-regulation of several ISGs (Figure 4C).

DNA and RNA cytosolic sensors trigger the IFN response with different specificity. Examples include MDA5 (IFIH1), RIG-I (DDX58), TLRs, cGAS or IFI16. These receptors activate intermediates such as MAVS (IPS-1) or STING that activate kinase TBK-1, which activates IRFs. We introduced shRNAs to deplete MDA5, TLR3, MAVS and STING from multiH1sh cells and observed a decrease in ISG stimulation upon Dox treatment (Figure 4D). Importantly, the factor that contributed the most to ISG up-regulation in multiH1 KD cells was MDA5, an RNA sensor, and the one that did it the least was STING, an adaptor of the DNA sensor pathway. Treating multiH1sh cells with 2-aminopurine, an inhibitor of IFN-inducible dsRNA-activated protein kinase R (PKR, EIF2AK2), which is involved in sensing dsRNA and activating MAVS, also impaired the activation of several ISGs (Figure 4C).

All together, these data show that upon H1 depletion an IFN response is being induced with participation of cytosolic sensors and signal transducers and features the synthesis of IFN, suggesting that some nucleic acid may be produced at the cytosol as a consequence of H1 depletion. Several genes involved in sensing and responding to foreign nucleic acids were up-regulated in multiH1 KD cells, including DDX60, IFI16, MDA5, RIG-I, LGP2, STAT1, IRF1, IRF7, IRF9, OASL and OAS2. Enrichment pathway analysis denoted that pathways like 'RIG-I/MDA5 (RNA sensing molecules)-mediated induction of IFN-alpha/beta' were significantly enriched, but not 'cytosolic sensors of pathogen-associated DNA', suggesting that the IFN response was being induced by RNA molecules upon multiH1 KD (data not shown).

Induction of repeats and endogenous retroviruses upon histone H1 knock-down

It has been previously reported that DNA methyltransferase inhibitors (DNMTis) induce the IFN response pathway in cancer cells with anti-proliferative effects by inducing synthesis of endogenous dsRNAs from endogenous retroviruses, DNA repeats and non-coding transcripts (60–62). We hypothesized that spurious transcription could be taking place from non-coding RNA genes, DNA repeats, satellites or endogenous retroviruses (ERVs), which are generally located in heterochromatin, and are sensed as foreign thus activating the IFN response.

Expression of several repeats was assessed by RT-qPCR in T47D multiH1sh cells upon Dox treatment, using random shRNA cells as a control (Figure 5). Some repeats were chosen because were found up-regulated in our multiH1sh RNAseq data (MER4D, HERVK and LTR57) (data not shown). Others were selected due to its high abundance of histone H1 variants according to our ChIP-seq data (MLT1J2) (data not shown, (25)). Expression of the endogenous retroviruses (ERVs) MER4D, MER21C, MLT1C49, HERVK, Env-Fc1, LTR57, MER25A and MLT1J2, the subtelomeric repeat D4Z4 and satellite A, are shown to be up-regulated to different extent upon multiH1 inhibition, but not in control treatment (Figure 5A). Up-regulation of these repeats was also observed in H1.4 + H1.2 combined KD cells, but not as much in individual H1 KDs (Figure 5B). Although some repeats are induced to some extent in individual H1 KDs, this is insufficient to trigger the IFN response. Higher induction of a wider number of repeats achieved with the double KD may be the cause of the IFN pathway stimulation observed.

To test that expression of ERVs is the origin of IFN signaling activation, we tested whether inhibition of retrotranscriptase (RT) activity affected the up-regulation of ISGs in multiH1 KD cells. MultiH1sh cells were treated for 3 days with doxycycline and a cocktail of RT inhibitors (Tenofovir 0.5 μM, Nevirapine 17 μM, Emtricitabine 7.3 μM). ISGs were induced similarly in the presence of RT inhibitors (data not shown), indicating that cDNA synthesis is not required and confirming that RNA could be the triggering molecule.

According to our data, a plausible model on how multiple H1 KD induces the IFN response would be that H1 depletion from heterochromatin may induce several non-coding RNAs from endogenous retroviruses, satellite and other repeats, that are sensed in the cytosol as exogenous (ds)RNAs. Immunofluorescence with the specific antibody J2 denoted that dsRNA was accumulated into the cytosol of multiH1sh cells upon doxycycline treatment (Figure 5C). Furthermore, analysis of the distribution of RNAseq reads in multiH1 cells demonstrates that upon H1 inhibition the proportion of intergenic and intronic reads respect to exonic reads was increased significantly (ca. 16% and 30%, respectively) (Figure 5D). This suggests that H1 depletion increases transcriptional noise, which may favor the accumulation of unexpected RNAs.

H1 abundance at genes deregulated by H1 depletion corresponds to its basal expression level

Additionally, H1 could accumulate at the ISG promoters for repression in the absence of IFN signaling, and severe H1 depletion could be enough to induce several of those genes (as reported elsewhere (63)), including IFN-encoding genes, mimicking an IFN-like response. Using our previously generated ChIP-seq data on H1 variants distribution in T47D cells (25), we analyzed H1 abundance at promoter and coding regions of multiH1sh regulated genes compared to total genes. Genes up- or down-regulated in multiH1 KD cells are not enriched in any particular H1 variant compared to the total genes of the genome, although some H1s including H1.2 are more abundant in up- than down-regulated genes, which likely accounts for the fact that H1.2 is the vari-

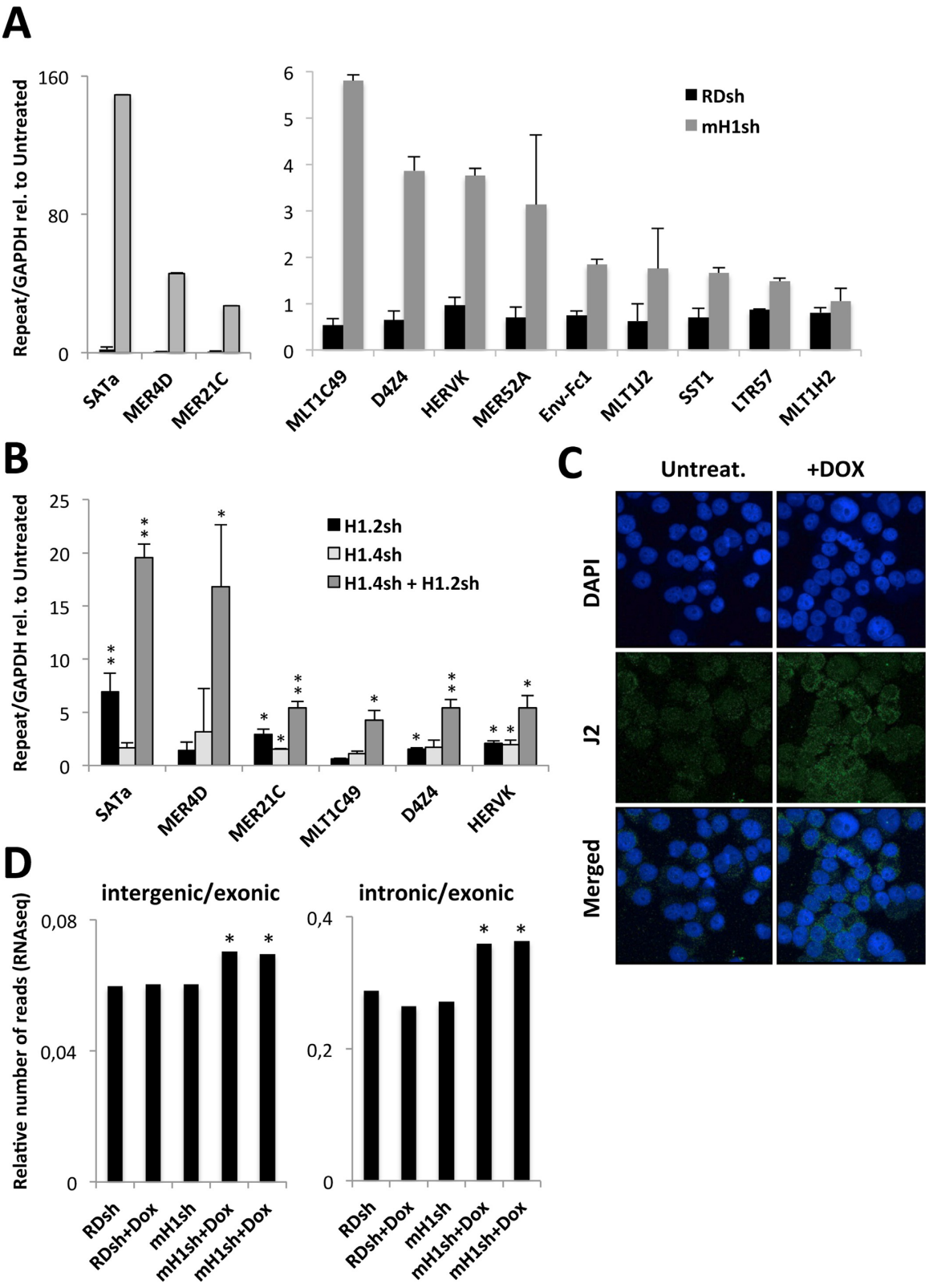

Figure 5. Expression of repetitive DNA upon histone H1 knock-down. (**A**) T47D cells containing RDsh or multiH1sh were treated or not with Dox for 3 days and expression of several repeats and endogenous retroviruses were tested by RT-qPCR. Expression in response to Dox is expressed corrected by GAPDH and relative to untreated cells. (**B**) T47D cells containing H1.2sh, H1.4sh or H1.4/H1.2sh were treated with Dox for 3 days and expression of repeats was tested and represented as in (A). Values represent the mean and SD of representative experiments performed in duplicate. Significance was tested using a *t*-test (**P*-value<0.05; ***P*-value < 0.01). (**C**) Accumulation of dsRNA in multiH1sh cells. Cells were treated or not with Dox for 6 days and submitted to immunofluorescence staining of dsRNA using J2 antibody. DAPI was used to stain the nucleus. (**D**) Relative number of intergenic or intronic RNAseq reads compared to exonic reads in RDsh or multiH1sh treated or not with Dox. Asterisks mark significance ($P < 2e{-}16$) in Dox-treated compared to untreated.

ant that better correlates negatively with gene expression (25), and up-regulated genes present lower basal gene expression as shown in Figure 2G (Supplementary Figure S7B and C). Interestingly, genes within the up-regulated gene set that show the highest responsiveness to IFN according to the Interferome data base, presented a lower basal gene expression average and a higher H1 content around the TSS (data not shown).

H1 variant ChIP-seq signals were similar around TSS of genes (25) up- and down-regulated genes in multiH1sh (Figure 6B and Supplementary Figure S7D). Both sets of genes showed H1.2 depletion around the TSS. Instead, H1.0 and H1.4 showed a local enrichment 1-kb at each side of the TSS of up-regulated genes, while down-regulated genes showed an average depletion of H1 around the TSS. Overall, H1 was more abundant in up-regulated genes, although not as high as in non- or lowly-expressed genes.

Genes highly responsive to multiH1sh and IFN may be tightly repressed with participation of H1.2 or H1.4 (among other variants) and, as a consequence, severe H1 depletion may render these genes open for transcription to take place. An open question is what makes these genes particular for being up-regulated upon H1 depletion. We randomly selected a subset of genes that remained repressed upon H1 reduction and analyzed the content of H1.2 in their proximal promoters. We found that H1 content at up-regulated genes was not significantly different to genes with low expression levels (Supplementary Figure S7E) and indeed H1 content most consistently correlated to expression levels in the absence of doxycycline. In conclusion, an increased H1 content does not seem to be the reason for up-regulation upon H1 depletion.

Gene activation by H1 depletion occurs without canonical marks of active chromatin

We next analyzed H1 variant levels at gene promoters by ChIP-qPCR. We found that H1.2 was present and being removed equally from up-regulated ISGs and uninduced (control) genes upon multiH1 KD, as well as from several DNA repeats and ERVs analyzed (Figure 6A). H1X abundance remained unchanged upon doxycycline treatment, even at induced genes (ISGs and H1.0). As a control, decreased H1s at TSS of active genes (CDK2 and H1.0) compared to an upstream (–3 kb) region, was observed, but not for a repressed gene (NANOG).

In parallel, we analyzed changes in core histone modifications related to gene expression and open chromatin (H3 and H4 pan-acetylation, and H3K4me3), or repression and closed chromatin (H3K9me3, H3K27me3 and H4K20me3). In general, active marks were present at active genes and absent from repeats, as expected. Repressive marks were more abundant at repeats and NANOG. Interestingly, H1.0 activation upon multiH1 KD was only marked by histone acetylation at TSS, but not H3K4me3. In contrast, all histone marks remained unaltered at TSS of all the ISGs analyzed that get activated upon multiH1 KD (Dox treatment) (Figure 6A). This is particularly puzzling for the canonical transcription initiation-associated mark H3K4me3. Differences between ISGs existed, but were not increased with Dox. Repressive marks were also mainly unaltered, and the same happened within repeats. We have previously reported that genes strongly up-regulated upon H1X KD did not present an H1 valley nor H3K4me3 increase at TSS (24), suggesting that gene activation by H1 depletion may occur without canonical marks of active chromatin, as recently reported to occur in certain genes (64). How the ISGs become activated upon H1 depletion without changes in histone marks remains elusive. Activation could be mediated by recruitment of activated IRFs into ISG promoters where active marks are already constitutive and H1 is depleted. It is noteworthy that in an experiment of treatment with IFN-ß, active marks were also not observed to be increased (data not shown).

We also analyzed whether these marks were altered globally by western blot on chromatin extracts. H3K9me3 and H3K27me3 marks were not altered, although HP1α signal was decreased in multiH1 KD cells (Figure 6C). H1.4 with the K26me3 post-translational modification has been proposed to bind the heterochromatin protein HP1α (21,32), suggesting H1.4 depletion could have an effect on chromatin-bound HP1, potentially impacting heterochromatin integrity and repeat repression.

Changes in chromatin accessibility upon H1 depletion

We have also analyzed changes in chromatin accessibility upon multiH1 KD. We assessed chromatin accessibility by ATAC-seq in T47D multiH1sh upon Dox treatment compared to untreated. As a control, accessibility at TSS of genes with unchanged expression was analyzed. Genes highly expressed showed more accessibility than poorly expressed genes (Figure 7A). Genes up and down-regulated in multiH1 KD cells showed slightly different accessibility levels at TSS, and only up-regulated genes showed increased TSS accessibility upon H1 KD (Figure 7B). Next, we searched for peaks of increased accessibility in Dox-treated multiH1sh cells compared to untreated cells within the genome-wide ATAC-seq data. Then, we calculated whether up or down-regulated genes presented an increased number of such newly accessible peaks compared to permutations of randomized genes. Up-regulated genes showed a tendency to have increased number of accessibility peaks both at their promoter and coding regions (P-value = 0.17 and 0.06, respectively), in agreement with its increased transcriptional state in multiH1 KD cells. Conversely, down-regulated genes showed reduced accessibility (P-value = 0.18 and 0.03 for promoter and coding regions, respectively).

Finally, we computed the genomic distribution of accessibility peaks and whether peaks were enriched within some category of repetitive DNA. Upon H1 depletion, accessibility peaks were enriched within introns and distal intergenic regions (Figure 7C), and at satellites, rDNA and simple repeats (Figure 7D). Among satellites where peaks were found enriched, we found SATa and SST1 which were up-regulated upon multiH1 KD (Figure 5A). These results support the notion that H1 depletion generates regions of open chromatin, including regions where repeats were repressed, that might generate synthesis of (ds)RNAs that are sensed at cytoplasm and induce the IFN signaling response.

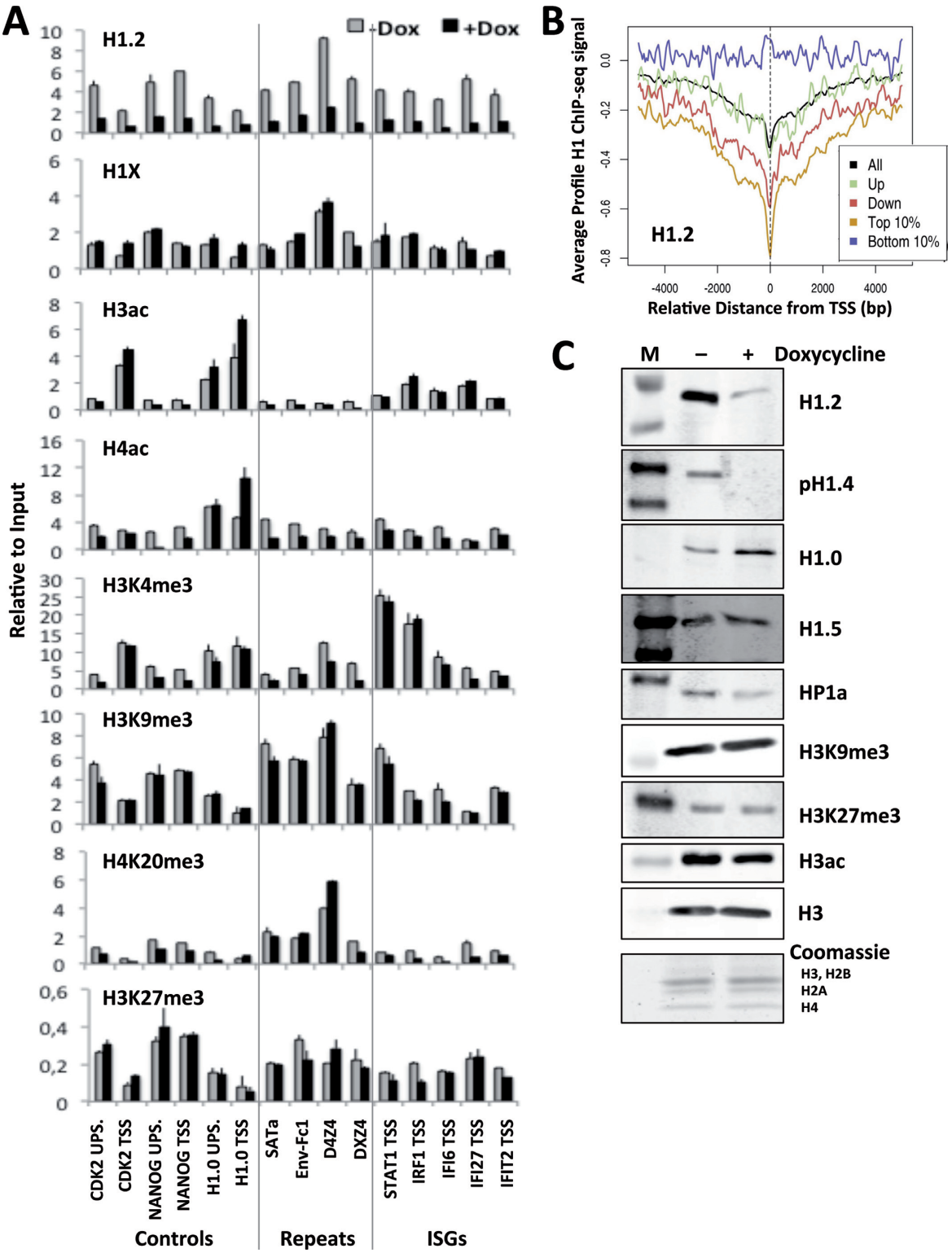

Figure 6. Changes at ISG promoters and chromatin upon H1 depletion. (**A**) Histone modification changes at promoters upon multiH1 KD. T47D cells containing multiH1sh were treated or not with Dox for 6 days and chromatin was extracted and immunoprecipitated (ChIP) with the indicated antibodies. Abundance at specific genomic regions (ISGs, DNA repeats and control genes) was quantified by real-time PCR and expressed relative to input DNA amplification. Oligonucleotides at the indicated promoters correspond to TSS or -3kb distal promoter (UPS). Values represent the mean and SD of a representative experiment performed in duplicate. (**B**) H1.2 abundance at TSS of deregulated genes. Average density profile of H1.2 abundance (input-subtracted ChIP-seq signal) around the TSS of up- or down-regulated genes upon multiH1 KD. RefSeq genes (All), as well as bottom and top 10% expressed genes (groups 1 and 10 in Supplementary Figure S7A), are shown as reference. (**C**) Chromatin-bound HP1α is decreased upon multiH1 KD. T47D cells containing multiH1sh were treated with Dox for 6 days and chromatin was extracted and immunoblotted with the indicated antibodies. Coomassie staining of core histones is shown.

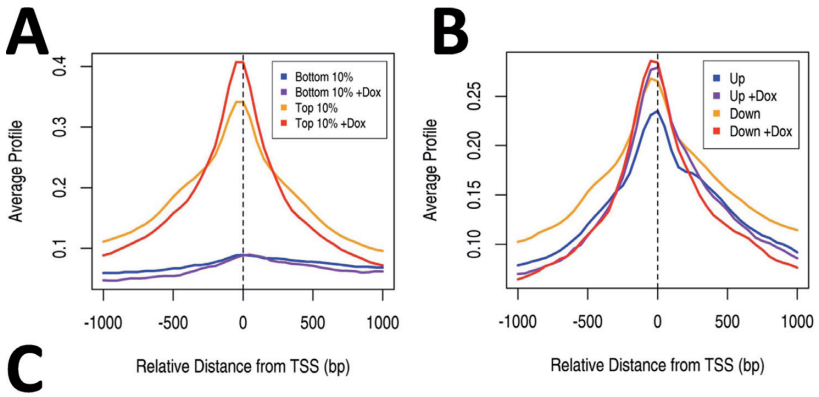

C

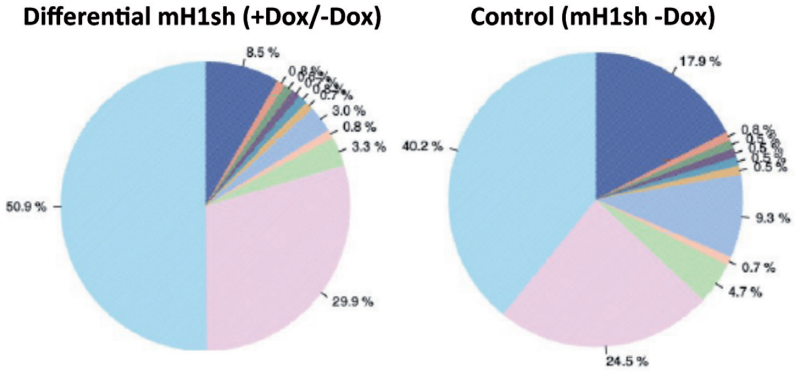

	Differ. +Dox/-Dox	Control -Dox	Genome
Promoter (<1000 bp)	8,5	17,9 *	1,1
Promoter (1000-2000 bp)	0,8	0,8	0,7
Promoter (2000-3000 bpp)	0,6	0,5	0,6
Downstream (<1000 bp)	0,7	0,5	0,9
Downstream (1000-2000 bp)	0,8 *	0,5	0,7
Downstream (2000-3000 bp)	0,7	0,5	0,6
5'UTR	3	9,3 *	0,4
3'UTR	0,8	0,7	1,4
Coding exon	3,3	4,7 *	1,9
Intron	29,9 *	24,5	41,6
Distal intergenic	50,9 *	40,2	50

*p-value<0,001

D

Repeat category	No.of peaks	
DNA	354	
LINE	1258	
Low_complexity	1073	*
LTR	1282	
Other	166	*
RC	1	
RNA	0	
rRNA	25	*
Satellite	3551	*
scRNA	0	
Simple_repeat	3866	*
SINE	2016	
snRNA	4	
srpRNA	4	
tRNA	9	
Unknown	0	

Satellites	No.of peaks
ALR/Alpha	966
(CATTC)n	580
CER	26
D20S16	124
(GAATG)n	1074
GSAT	55
GSATII	159
GSATX	41
HSAT4	20
HSATII	368
MSR1	19
SATR1	41
SST1	24
TAR1	12

Figure 7. Changes on chromatin accessibility upon depletion of histone H1. T47D cells containing multiH1sh were treated or not with Dox for 6 days and submitted to ATAC-seq. (A and B) Average profiles of accessibility around the center of TSS, normalized to reads depth, for the following groups of genes: bottom and top 10% expressed genes (groups 1 and 10 in Supplementary Figure S7A) (**A**), and up- and down-regulated genes in multiH1 KD cells (**B**). (**C**) Genomic annotation of high accessibility regions (narrow peaks) enriched in multiH1sh Dox-treated compared to untreated cells, shown as pie diagram and table (% of total). For comparison, the genomic annotation of accessibility sites in control cells (untreated) is shown. Asterisks mark genomic categories enriched in differential mH1sh accessibility peaks compared to control or vice versa (P-value < 0.001). (**D**) Distribution of high accessibility peaks enriched in multiH1sh cells among the different annotated categories of genomic DNA repeats. Asterisks mark those repeat categories where the number of peaks obtained is significantly higher (P-value < 0.001) than expected in randomized samples (10^4 permutations) mimicking the accessibility peaks file. Within the satellite category, types that were significantly enriched are shown in the right panel.

Low expression of replication-dependent H1 variants in pancreatic adenocarcinomas over-expressing genes of the IFN pathway

Seeing a potential link between H1 variant levels and activation of the IFN response, we looked for other models in which this link may be apparent. Resistance to oncolytic viral therapy in pancreatic adenocarcinomas and multiple myelomas has been associated with overexpression of the anti-viral innate immune response (65). Monsurrò *et al.* identified two molecular phenotypes of pancreatic cancer characterized by a differential expression of genes associated with IFN signaling (66). We have constructed a cluster dendrogram of the expression of IFN signaling related genes in pancreatic cancer and normal samples obtained from databases that has defined three groups of samples, where group 1 contain mainly normal samples and groups 2 and 3 contain most tumor samples (Supplementary Figure S8). Groups 2 and 3 show overall up-regulation of IFN-related genes compared to group 1, while no differences in expression of randomly chosen genes exist among groups (Figure 8). Next we plotted the expression of H1 variants in all the samples of the three groups, and observed that many replication-dependent H1 variants are down-regulated in sample groups presenting ISGs up-regulation, while replication-independent variants are up-regulated, resembling the situation in our T47D multiple 'replication-dependent' H1 KD where ISGs are up-regulated.

However, most cancer types show an up-regulation of H1-encoding genes compared to normal tissue, including breast carcinoma (10). An interesting reported exception is the low H1.2 expression in colorectal cancer compared to normal tissue. ISG expression was not increased in colorectal cancer compared to normal samples despite of the low H1.2 expression in cancer samples, indicating that the correlation in pancreatic cancer does not extend to colorectal cancer where only H1.2 is down-regulated (data not shown). This is consistent with our results, wherein we only register an IFN response in multi-variant down-regulation.

DISCUSSION

This work extends our research on the biological effects of depleting histone H1 variants in cancer cells, by adding shRNA-expressing vectors against H1.4 and simultaneous depletion of several variants with a single shRNA (multiH1), or combining shRNAs. We reported before that individual H1 KDs alter expression of small subsets of genes in T47D cells, with little overlap between variants. Knocking-down individual variants affects proliferation to different degrees. Our experiments show that any H1 variant KD is unable to completely impair cell growth, whether because depletion is incomplete or because H1 variants present some redundancy. Instead, simultaneous depletion of multiple H1 variants has drastic consequences on cell proliferation. We have tested different combinations of H1 KDs, and found co-KD of H1.2 + H1.4 to be the combination with greatest inhibition of cell growth (data not shown). Our results suggest that these two variants are most important for cell homeostasis. Either the two variants play redundant roles, or the observed consequences of multiH1s are due to the additive effects of impairing H1.2 and H1.4 non-redundant functions. Because distribution of H1.2 and H1.4 in the genome is not redundant (25), we favor the second explanation.

Nonetheless, the gene expression profile of multiH1 KD cells is not explained by simple addition of the H1.2 and H1.4 KD profiles. Combination of gene expression profiling and ChIP-seq data of H1s variants fails to show that these genes are specifically targeted and directly regulated by the corresponding variant. Multiple H1 KD present a considerable number of genes deregulated; roughly, 3-times the number of the sum of genes deregulated in H1.2 and H1.4 single KDs. Interestingly, a big proportion of genes, in particular the strongest up-regulated genes, are related to the IFN response. It is worth mentioning that genes up-regulated upon multiH1 KD are genes that are silenced under basal conditions. The opposite is true for the down-regulated genes. As before, we do not support the hypothesis that all these ISGs are maintained repressed particularly by H1.2 and H1.4, as others have suggested (63). Although we have found that H1s are enriched in the promoter and coding regions of genes up-regulated in multiH1 KD compared to other genes, we show that this H1 content is characteristic of genes presenting that low basal expression rates and do not represent especially silenced H1 targets. We have shown before that H1 content correlates positively with gene silencing in T47D, with H1.2 having the highest degree of correlation (24,25).

We believe ISG induction in multiH1 KD may be caused by the production and cytosolic sensing of unusual nucleic acids, and secondarily through the synthesis of IFN. We show here that several intermediate components of the IFN signaling pathway are up-regulated upon doxycycline treatment of multiH1 KD cells, type-I IFN is being expressed and liberated to the media, and ISG stimulation is depending on the presence of several pathogen recognition receptors (MDA5, TLR3) and adaptor molecules (MAVS, STING), on type-I IFN receptors, and on TBK and JAK activation.

Several recent reports have shown that DNMT inhibitors with anti-proliferative effects induce the IFN response pathway in cancer cells by inducing synthesis of dsRNAs from endogenous retroviruses, DNA repeats and non-coding transcripts (60–62). The striking similarity of these reports with our observations led us to investigate whether multiH1 depletion was leading to spurious transcription from non-coding RNA genes, DNA repeats, satellites or endogenous retroviruses (ERVs), generally located in heterochromatin. Enrichment pathway analysis of our multiH1 KD expression data indicated that the IFN response is induced by RNA transcripts, not by DNA, as only genes belonging to the RNA-sensing pathway are up-regulated. Accordingly, we detected expression of satellite repeats and ERVs that might be induced upon heterochromatin relaxation. Fittingly, both variants depleted by our multiH1sh have been associated with maintaining heterochromatin. First, H1.4 has been suggested to associate with heterochromatin through its ability to recruit HP1, L3MBTL1 and polycomb proteins through H1.4K26me (21,22,32,33,67,68). H1.2 may have multiple roles, as it has been associated with active transcription and repression and in complex with different partners (30,31,69). In T47D cells, we have charac-

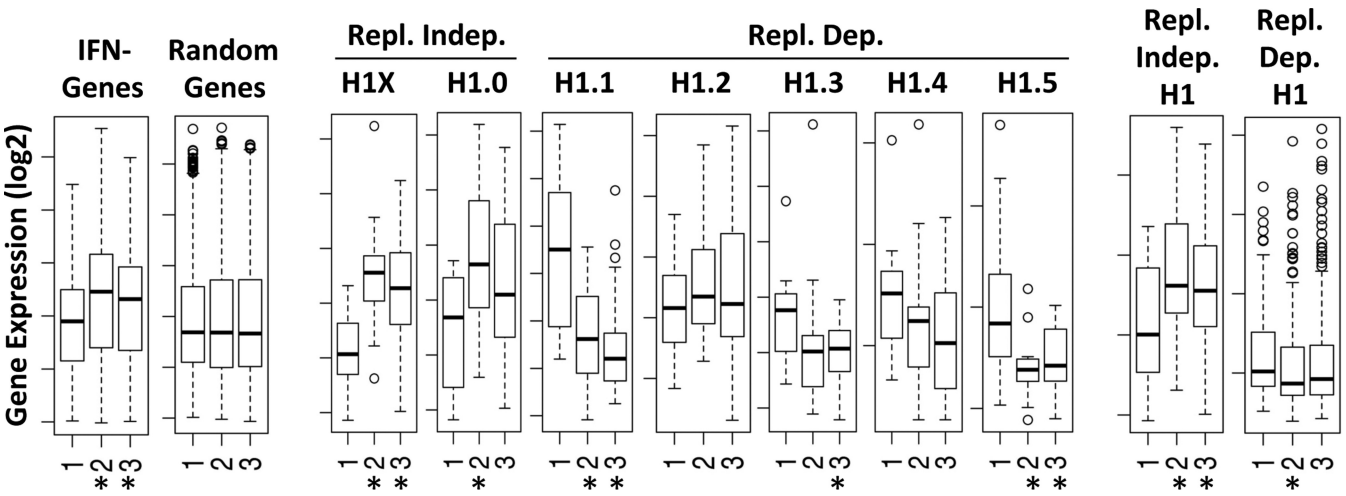

Figure 8. H1 expression in pancreatic normal and cancer samples clustered according to the expression of IFN signaling related genes. Supervised cluster analysis of IFN related genes in 36 pancreatic tumor and 16 normal samples using microarray data deposited in GSE16515, defined 3 groups of samples (see Supplementary Figure S8). Box plots represent the expression of IFN related genes and H1 variants, ether individually or grouped as replication dependent or independent H1s, in the three groups of samples. Expression of a representative set of genes chosen randomly is shown as a control. Significance was assessed using the Kolmogorov-Smirnov test. Significant difference between groups 2 or 3 and group 1 is marked with asterisks ($P < 0.05$). Relative expression units have been omitted for simplicity.

terized H1.2 as enriched within lamin-associated domains (LADs), intergenic regions, repressed chromatin and gene-poor chromosomes (25).

We have tried to establish whether derepression of repeats and induction of the IFN response is due to overall decrease on the H1 content, or to the specific depletion of H1.2 + H1.4. Single KD of these variants does not cause these effects in T47D cells. Other double KD combinations are less effective (H1.2 + H1.5) or ineffective (H1.4 + H1.5). This would suggest that H1.2 is important to maintain repression, but not sufficient alone, and requires H1.4 also participating.

An alternate hypothesis is that total H1 content could be the key determinant of the observed multiH1 KD effects. Indeed, up-regulation of ISGs in T47D multiH1 KD was complemented equally by H1.2, H1.3 or H1.4 overexpression, going against the notion that H1.2 is essential, and favoring redundancy between variants. We reported elsewhere the approximate content of H1 variants in T47D cells, representing H1.2, H1.4 and H1.5, 20–30% of the total H1 content each (26). Then, assuming complete depletion, H1.2 + H1.4 inhibition should not represent a decrease on the total H1 content larger than the inhibitions H1.2 + H1.5, or H1.4 + H1.5. In fact, Coomassie staining of histone extracts has shown that total H1 content was reduced to 70–80% of wild-type in multiH1 or H1.4/H1.2 KD cells. H1 content reduction in the other double KDs (H1.2/H1.5 and H1.4/H1.5) we generated was comparable (down to 60–80%) despite of incomplete H1.5 depletion. Furthermore, simultaneous depletion of H1.3/H1.4/H1.5 rendered ISGs unaltered. In conclusion, the observed effects are better explained by the specificity of H1.2 and H1.4 functions than by the reduction of overall H1 content.

Because total H1 content and the abundance or distribution of the different variants may differ between cell types, KD of single or multiple variants may have different outcomes within different models. Despite of this, we have detected ISG induction also in MCF7 multiH1 KD cells. Interestingly, by analyzing publically available transcriptomic data, we have detected ISG up-regulation in H1.2 (and EZH2) KD experiments performed by another group in MCF7 (31) and 293T cells (30) (data not shown), although induction of the IFN response was not reported in those studies. Both data sets show a better overlap with our T47D multiH1sh up-regulated genes subset than with the H1.2sh up-regulated genes. This indicates that H1 variant depletion has different transcriptional effects in different cell types, and H1.2 depletion is not sufficient to induce the IFN response in T47D cells but induces to some extent several ISGs in HeLa (see below) (63), MCF7 and 293T, further arguing in favor of a special role for H1.2. All together these studies confirm the notion that H1 depletion may trigger this innate immune response in several cell types.

Single and double H1 knock-outs (KO) in mice have limited effects due to compensation and redundancy, but drastic effects were observed in triple KO (TKO) embryos and MEFs due to reduction of H1 total content to 50% (27,36,37). Yang *et al.* demonstrated that some H1 subtypes specifically interact with the DNA methyltransferases DNMT1 and DNMT3B to promote methylation of imprinted genes, which become up-regulated in mouse TKO (27,38). Major satellites are also up-regulated in mouse TKO (39), and because DNMTis induce the IFN response pathway in cancer cells by inducing synthesis of DNA repeats (60–62), we hypothesized that multiple H1 depletion in breast cancer cells could lead to DNMTs displacement and demethylation of heterochromatic repeats leading to IFN signaling. Then, treatment with DNMTis and H1 depletion would have similar effects. Treatment of T47D cells with 5-aza-2′-deoxycytidine (aza-dC) for 3 days did not induce the expression of ISGs, but enhanced the effect of multiH1 KD (Supplementary Figure S9). Response of the DNA

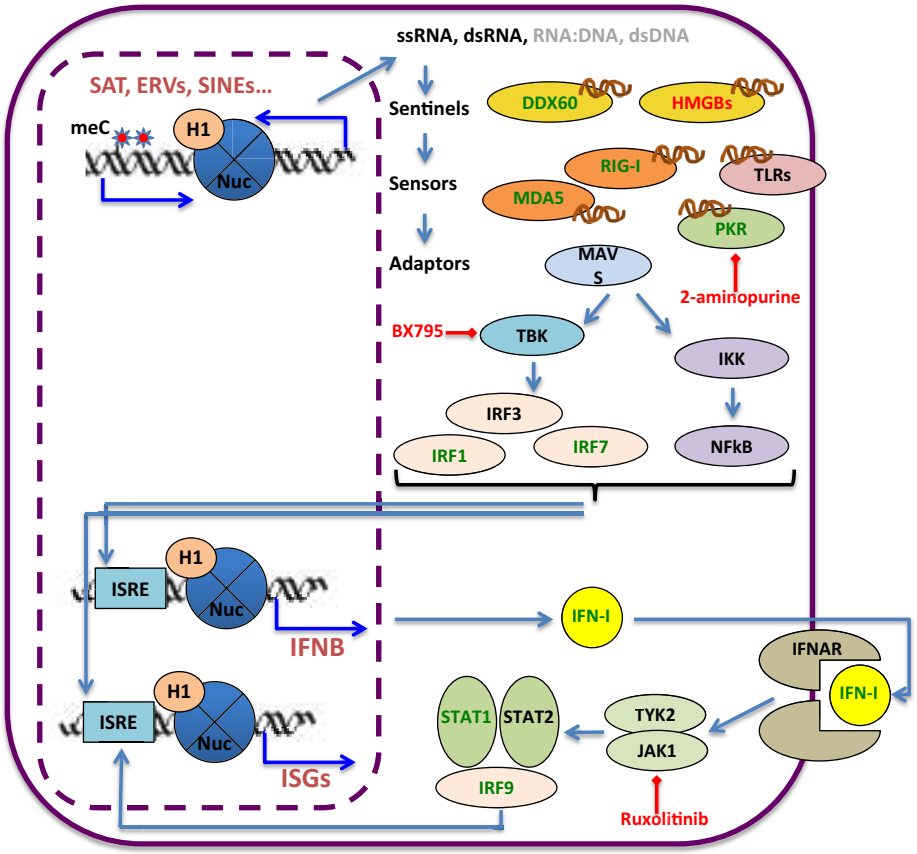

Figure 9. Model of H1 involvement in the repression of the interferon response. Histone H1 participates in the repression of strongly silenced genes such as ISGs under basal conditions, and in the repression of non-coding transcripts derived from repeats such as satellites, transposons and endogenous retroviruses located in heterochromatic regions which may cause, upon induction in H1-depleted cells, activation of the IFN signaling pathway. Transcription of repeats may give raise to ss/dsRNAs (60–62) or non-B DNA structures such as R-loops (70), that could be sensed by universal (HMGBs) or ligand-specific cytosolic sentinels (DDX60) that activate RNA (MDA5/IFIH1, RIG-I, LGP2, OASs) or DNA sensors (cGAS, IFI16), or by membrane-associated Toll-like receptors (TLRs). These proteins transduce the signal to specific adaptors (MAVS/IPS1, STING), leading to the activation of TBK-IRFs and IKK-NFkB. These transcription factors bind specific sites at ISG promoters, including genes for the synthesis of type I IFN that upon interaction with specific receptors lead to the activation of JAK-STAT pathway and additional IRFs. For simplicity, few of the sensor and adaptor proteins are drawn. ISGs up-regulated in multiH1 KD cells include DDX60, MDA5/IFIH1, RIG-I/DDX58, LGP2, PKR, OAS1/IFI4, OAS2, OASL, IRF1, IRF7, IRF9, IFNB, STAT1 (in green). HMGB1, HMGB2 and HMGB3 are down-regulated. Inhibitors of members of the IFN signaling pathway are shown (in red).

repeats to aza-dC was heterogeneous (data not shown). So, in T47D cells, DNMTis do not induce ISGs nor repeats as observed in multiH1 KD, so we do not favor the model in which the effects observed upon H1 depletion are mediated only by DNA demethylation. Nonetheless, it was interesting to address the global methylation state of DNA in multiH1 KD cells. In this direction, we have evaluated changes on global DNA methylation upon multiH1 KD with a genome-wide CpG array that showed virtually no differentially methylated CpGs after six days of doxycycline treatment. Methylation of several ERV elements was also analyzed by bisulphite PCR and changes were not found (Supplementary Figure S9).

Due to all evidences reported here, we favor a model in which histone H1 participates in the repression of genes such as ISGs under basal conditions, and in the repression of non-coding transcripts derived from repeats such as satellites, transposons and endogenous retroviruses located in heterochromatic regions which may cause, upon induction in H1-depleted cells, activation of the IFN response (Figure 9). We have directly observed the increase of cytosolic dsRNA within multi H1 KD cells, increased expression of satellites and repeats, enhanced accumulation of RNAseq reads from intergenic and intronic regions, and increased chromatin accessibility of all these regions. It has been previously shown that tumor cells may contain retroelements-derived DNA in the cytosol forming structures including R-loops, whose levels are increased by genotoxic agents, which activate the IFN response (70). We cannot disregard the possibility that upon expression of repeat elements, R-loops are formed and RNA:DNA or triple stranded fragments are detected in the cytosol by sensors that induce the IFN pathway (71). Overall, our data suggest that activation of ISGs by H1 KD is mediated by activating the IFN signaling pathway, rather than by direct promoter relaxation due to H1 displacement.

ChIP analysis of ISG promoters upon multiH1 KD has shown that active marks are not increased as it would be expected for genes that are induced strongly. It has been recently reported that developmental genes are activated

in the absence of positive marks with the participation of program-specific transcription factors (TFs), allowing rapid activation and deactivation (64). ISGs may fall in this category, where clearance of histone H1, together with binding of IRFs and NFkB to the promoters, may be sufficient for activation. Forced depletion of H1 may be enough to create a permissive chromatin environment to allow transcription without the need of the contribution of active histone marks. Despite of this, H1 clearance may not be sufficient without upstream induction of the IFN signaling pathway that activate NFkB and IRFs to bind to the ISG promoters. This may explain why the control genes analyzed (and the large proportion of the transcriptome), that also show H1.2 clearance, are not induced upon multiH1 KD, favoring the model that IFN signaling is required. Moreover, our ChIP data and data extracted from the UCSC browser shows that many ISGs present significant amounts of H3K4me3 under basal conditions. This is a particularity of genes that respond rapidly to stimulus, and may explain why upon induction these genes do not show increased levels of this mark, neither upon IFN-ß treatment.

A role of H1 in the regulation of ISGs has been suggested before. The H1 chaperone SET/TAF-I has been suggested to participate in the H1-mediated silencing of ISG15, ISG54, ISG56 (IFIT1) and IFITM1 in HeLa cells (63). In the absence of IFN, these genes were discretely up-regulated (two-fold, in average) not only in TAF-I KD but also in H1.2 KD cells. We have confirmed that TAF-I KD causes modest up-regulation of some ISGs in T47D cells (data not shown), but H1.2 KD does not in our hands, until combined with another H1 (H1.4) variant KD. Then, induction fold-changes are much higher (Figure 3A), further suggesting multiH1 KD induces ISGs not only due to its local contribution to promoter chromatin structure, but also inducing the IFN pathway upstream due to derepression of DNA repeats. Whether this IFN signaling is caused by heterochromatin instability and expression of repeats, originated in the altered H1 expression, DNA hypomethylation or other chromatin alterations, are appealing possibilities that need to be explored.

DATA AVAILABILITY

RNAseq data is available in the Gene Expression Omnibus (GEO) database under the accession number GSE83277. ATACseq data accession number is GSE100762.

SUPPLEMENTARY DATA

Supplementary Data are available Online.

ACKNOWLEDGEMENTS

We thank former members of the laboratory Regina Mayor, Jean-Michel Terme and Neus Luque for discussions, Alicia Roque for critical reading of the manuscript, and Marian Martínez-Balbas, Ferran Azorín and Jordi Bernués for sharing reagents and discussions. We thank Javier Martínez-Picado for sharing with us the RT inhibitors. We thank CRG and CNAG sequencing core facilities for the ATAC-seq and RNAseq experiments, respectively.

FUNDING

Spanish Ministry of Economy and Competitiveness (MINECO) and European Regional Development Fund [BFU2014–52237-P]. A.B. received a predoctoral fellowship from SENESCYT from Ecuador. M.D. was recipient of a fellowship from MINECO [PTA2014–09515-I]. A.E.-C. was funded by the RED-BIO project of the Spanish National Bioinformatics Institute (INB) [PT13/0001/0044]. The INB is funded by the Spanish National Health Institute Carlos III (ISCIII) and MINECO. Funding for open access charge: Spanish Ministry of Economy and Competitiveness (MINECO) and European Regional Development Fund [BFU2014-52237-P].
Conflict of interest statement. None declared.

REFERENCES

1. Bednar,J., Horowitz,R.A., Grigoryev,S.A., Carruthers,L.M., Hansen,J.C., Koster,A.J. and Woodcock,C.L. (1998) Nucleosomes, linker DNA, and linker histone form a unique structural motif that directs the higher-order folding and compaction of chromatin. *Proc. Natl. Acad. Sci. U.S.A.*, **95**, 14173–14178.
2. Pennings,S., Meersseman,G. and Bradbury,E.M. (1994) Linker histones H1 and H5 prevent the mobility of positioned nucleosomes. *Proc. Natl. Acad. Sci. U.S.A.*, **91**, 10275–10279.
3. Laybourn,P.J. and Kadonaga,J.T. (1991) Role of nucleosomal cores and histone H1 in regulation of transcription by RNA polymerase II. *Science*, **254**, 238–245.
4. Happel,N. and Doenecke,D. (2009) Histone H1 and its isoforms: contribution to chromatin structure and function. *Gene*, **431**, 1–12.
5. Izzo,A., Kamieniarz,K. and Schneider,R. (2008) The histone H1 family: specific members, specific functions? *Biol. Chem.*, **389**, 333–343.
6. Millan-Arino,L., Izquierdo-Bouldstridge,A. and Jordan,A. (2016) Specificities and genomic distribution of somatic mammalian histone H1 subtypes. *Biochim. Biophys. Acta*, **1859**, 510–519.
7. Terme,J.M., Sese,B., Millan-Arino,L., Mayor,R., Izpisua Belmonte,J.C., Barrero,M.J. and Jordan,A. (2011) Histone H1 variants are differentially expressed and incorporated into chromatin during differentiation and reprogramming to pluripotency. *J. Biol. Chem.*, **286**, 35347–35357.
8. Pan,C. and Fan,Y. (2016) Role of H1 linker histones in mammalian development and stem cell differentiation. *Biochim. Biophys. Acta*, **1859**, 496–509.
9. Sato,S., Takahashi,S., Asamoto,M., Nakanishi,M., Wakita,T., Ogura,Y., Yatabe,Y. and Shirai,T. (2012) Histone H1 expression in human prostate cancer tissues and cell lines. *Pathol. Int.*, **62**, 84–92.
10. Scaffidi,P. (2016) Histone H1 alterations in cancer. *Biochim. Biophys. Acta*, **1859**, 533–539.
11. Medrzycki,M., Zhang,Y., McDonald,J.F. and Fan,Y. (2012) Profiling of linker histone variants in ovarian cancer. *Front. Biosci. (Landmark Ed.)*, **17**, 396–406.
12. Meergans,T., Albig,W. and Doenecke,D. (1997) Varied expression patterns of human H1 histone genes in different cell lines. *DNA Cell Biol.*, **16**, 1041–1049.
13. Parseghian,M.H. and Hamkalo,B.A. (2001) A compendium of the histone H1 family of somatic subtypes: an elusive cast of characters and their characteristics. *Biochem. Cell Biol.*, **79**, 289–304.
14. Zhang,Y., Cooke,M., Panjwani,S., Cao,K., Krauth,B., Ho,P.Y., Medrzycki,M., Berhe,D.T., Pan,C., McDevitt,T.C. *et al.* (2012) Histone h1 depletion impairs embryonic stem cell differentiation. *PLoS Genet.*, **8**, e1002691.
15. Torres,C.M., Biran,A., Burney,M.J., Patel,H., Henser-Brownhill,T., Cohen,A.S., Li,Y., Ben-Hamo,R., Nye,E., Spencer-Dene,B. *et al.* (2016) The linker histone H1.0 generates epigenetic and functional intratumor heterogeneity. *Science*, **353**, aaf1644.
16. Kalashnikova,A.A., Rogge,R.A. and Hansen,J.C. (2016) Linker histone H1 and protein-protein interactions. *Biochim. Biophys. Acta*, **1859**, 455–461.

17. Izzo,A. and Schneider,R. (2016) The role of linker histone H1 modifications in the regulation of gene expression and chromatin dynamics. *Biochim. Biophys. Acta*, **1859**, 486–495.
18. Hergeth,S.P., Dundr,M., Tropberger,P., Zee,B.M., Garcia,B.A., Daujat,S. and Schneider,R. (2011) Isoform-specific phosphorylation of human linker histone H1.4 in mitosis by the kinase Aurora B. *J. Cell Sci.*, **124**, 1623–1628.
19. Kamieniarz,K., Izzo,A., Dundr,M., Tropberger,P., Ozretic,L., Kirfel,J., Scheer,E., Tropel,P., Wisniewski,J.R., Tora,L. *et al.* (2012) A dual role of linker histone H1.4 Lys 34 acetylation in transcriptional activation. *Genes Dev.*, **26**, 797–802.
20. Weiss,T., Hergeth,S., Zeissler,U., Izzo,A., Tropberger,P., Zee,B.M., Dundr,M., Garcia,B.A., Daujat,S. and Schneider,R. (2010) Histone H1 variant-specific lysine methylation by G9a/KMT1C and Glp1/KMT1D. *Epigenet. Chromatin*, **3**, 7.
21. Hale,T.K., Contreras,A., Morrison,A.J. and Herrera,R.E. (2006) Phosphorylation of the linker histone H1 by CDK regulates its binding to HP1alpha. *Mol. Cell*, **22**, 693–699.
22. Vaquero,A., Scher,M., Lee,D., Erdjument-Bromage,H., Tempst,P. and Reinberg,D. (2004) Human SirT1 interacts with histone H1 and promotes formation of facultative heterochromatin. *Mol. Cell*, **16**, 93–105.
23. Kim,K., Jeong,K.W., Kim,H., Choi,J., Lu,W., Stallcup,M.R. and An,W. (2012) Functional interplay between p53 acetylation and H1.2 phosphorylation in p53-regulated transcription. *Oncogene*, **31**, 4290–4301.
24. Mayor,R., Izquierdo-Bouldstridge,A., Millan-Arino,L., Bustillos,A., Sampaio,C., Luque,N. and Jordan,A. (2015) Genome distribution of replication-independent histone H1 variants shows H1.0 associated with nucleolar domains and H1X associated with RNA polymerase II-enriched regions. *J. Biol. Chem.*, **290**, 7474–7491.
25. Millan-Arino,L., Islam,A.B., Izquierdo-Bouldstridge,A., Mayor,R., Terme,J.M., Luque,N., Sancho,M., Lopez-Bigas,N. and Jordan,A. (2014) Mapping of six somatic linker histone H1 variants in human breast cancer cells uncovers specific features of H1.2. *Nucleic Acids Res.*, **42**, 4474–4493.
26. Sancho,M., Diani,E., Beato,M. and Jordan,A. (2008) Depletion of human histone H1 variants uncovers specific roles in gene expression and cell growth. *PLoS Genet.*, **4**, e1000227.
27. Fan,Y., Nikitina,T., Zhao,J., Fleury,T.J., Bhattacharyya,R., Bouhassira,E.E., Stein,A., Woodcock,C.L. and Skoultchi,A.I. (2005) Histone H1 depletion in mammals alters global chromatin structure but causes specific changes in gene regulation. *Cell*, **123**, 1199–1212.
28. Shen,X. and Gorovsky,M.A. (1996) Linker histone H1 regulates specific gene expression but not global transcription in vivo. *Cell*, **86**, 475–483.
29. Lin,Q., Inselman,A., Han,X., Xu,H., Zhang,W., Handel,M.A. and Skoultchi,A.I. (2004) Reductions in linker histone levels are tolerated in developing spermatocytes but cause changes in specific gene expression. *J. Biol. Chem.*, **279**, 23525–23535.
30. Kim,K., Lee,B., Kim,J., Choi,J., Kim,J.M., Xiong,Y., Roeder,R.G. and An,W. (2013) Linker Histone H1.2 cooperates with Cul4A and PAF1 to drive H4K31 ubiquitylation-mediated transactivation. *Cell Rep.*, **5**, 1690–1703.
31. Kim,J.M., Kim,K., Punj,V., Liang,G., Ulmer,T.S., Lu,W. and An,W. (2015) Linker histone H1.2 establishes chromatin compaction and gene silencing through recognition of H3K27me3. *Sci. Rep.*, **5**, 16714.
32. Daujat,S., Zeissler,U., Waldmann,T., Happel,N. and Schneider,R. (2005) HP1 binds specifically to Lys26-methylated histone H1.4, whereas simultaneous Ser27 phosphorylation blocks HP1 binding. *J. Biol. Chem.*, **280**, 38090–38095.
33. Kuzmichev,A., Jenuwein,T., Tempst,P. and Reinberg,D. (2004) Different EZH2-containing complexes target methylation of histone H1 or nucleosomal histone H3. *Mol. Cell*, **14**, 183–193.
34. Krishnakumar,R., Gamble,M.J., Frizzell,K.M., Berrocal,J.G., Kininis,M. and Kraus,W.L. (2008) Reciprocal binding of PARP-1 and histone H1 at promoters specifies transcriptional outcomes. *Science (New York, N.Y.)*, **319**, 819–821.
35. Vicent,G.P., Nacht,A.S., Font-Mateu,J., Castellano,G., Gaveglia,L., Ballare,C. and Beato,M. (2011) Four enzymes cooperate to displace histone H1 during the first minute of hormonal gene activation. *Genes Dev.*, **25**, 845–862.
36. Fan,Y., Sirotkin,A., Russell,R.G., Ayala,J. and Skoultchi,A.I. (2001) Individual somatic H1 subtypes are dispensable for mouse development even in mice lacking the H1(0) replacement subtype. *Mol. Cell. Biol.*, **21**, 7933–7943.
37. Fan,Y., Nikitina,T., Morin-Kensicki,E.M., Zhao,J., Magnuson,T.R., Woodcock,C.L. and Skoultchi,A.I. (2003) H1 linker histones are essential for mouse development and affect nucleosome spacing in vivo. *Mol. Cell. Biol.*, **23**, 4559–4572.
38. Yang,S.M., Kim,B.J., Norwood Toro,L. and Skoultchi,A.I. (2013) H1 linker histone promotes epigenetic silencing by regulating both DNA methylation and histone H3 methylation. *Proc. Natl. Acad. Sci. U.S.A.*, **110**, 1708–1713.
39. Cao,K., Lailler,N., Zhang,Y., Kumar,A., Uppal,K., Liu,Z., Lee,E.K., Wu,H., Medrzycki,M., Pan,C. *et al.* (2013) High-resolution mapping of h1 linker histone variants in embryonic stem cells. *PLoS Genet.*, **9**, e1003417.
40. Geeven,G., Zhu,Y., Kim,B.J., Bartholdy,B.A., Yang,S.M., Macfarlan,T.S., Gifford,W.D., Pfaff,S.L., Verstegen,M.J., Pinto,H. *et al.* (2015) Local compartment changes and regulatory landscape alterations in histone H1-depleted cells. *Genome Biol.*, **16**, 289.
41. Wiznerowicz,M. and Trono,D. (2003) Conditional suppression of cellular genes: lentivirus vector-mediated drug-inducible RNA interference. *J. Virol.*, **77**, 8957–8961.
42. Perez Losada,A., Woessner,S., Sole,F., Florensa,L. and Bonet,C. (1994) Chromosomal and in vitro culture studies in a case of primary plasma cell leukemia. *Cancer Genet. Cytogenet.*, **76**, 36–38.
43. Dobin,A., Davis,C.A., Schlesinger,F., Drenkow,J., Zaleski,C., Jha,S., Batut,P., Chaisson,M. and Gingeras,T.R. (2013) STAR: ultrafast universal RNA-seq aligner. *Bioinformatics*, **29**, 15–21.
44. Li,B. and Dewey,C.N. (2011) RSEM: accurate transcript quantification from RNA-Seq data with or without a reference genome. *BMC Bioinformatics*, **12**, 323.
45. Love,M.I., Huber,W. and Anders,S. (2014) Moderated estimation of fold change and dispersion for RNA-seq data with DESeq2. *Genome Biol.*, **15**, 550.
46. Rusinova,I., Forster,S., Yu,S., Kannan,A., Masse,M., Cumming,H., Chapman,R. and Hertzog,P.J. (2013) Interferome v2.0: an updated database of annotated interferon-regulated genes. *Nucleic Acids Res.*, **41**, D1040–D1046.
47. Heinz,S., Benner,C., Spann,N., Bertolino,E., Lin,Y.C., Laslo,P., Cheng,J.X., Murre,C., Singh,H. and Glass,C.K. (2010) Simple combinations of lineage-determining transcription factors prime cis-regulatory elements required for macrophage and B cell identities. *Mol. Cell*, **38**, 576–589.
48. Young,M.D., Wakefield,M.J., Smyth,G.K. and Oshlack,A. (2010) Gene ontology analysis for RNA-seq: accounting for selection bias. *Genome Biol*, **11**, R14.
49. Supek,F., Bosnjak,M., Skunca,N. and Smuc,T. (2011) REVIGO summarizes and visualizes long lists of gene ontology terms. *PLoS One*, **6**, e21800.
50. Wu,G., Feng,X. and Stein,L. (2010) A human functional protein interaction network and its application to cancer data analysis. *Genome Biol.*, **11**, R53.
51. Shannon,P., Markiel,A., Ozier,O., Baliga,N.S., Wang,J.T., Ramage,D., Amin,N., Schwikowski,B. and Ideker,T. (2003) Cytoscape: a software environment for integrated models of biomolecular interaction networks. *Genome Res.*, **13**, 2498–2504.
52. Bao,W., Kojima,K.K. and Kohany,O. (2015) Repbase Update, a database of repetitive elements in eukaryotic genomes. *Mob. DNA*, **6**, 11.
53. Langmead,B., Trapnell,C., Pop,M. and Salzberg,S.L. (2009) Ultrafast and memory-efficient alignment of short DNA sequences to the human genome. *Genome Biol.*, **10**, R25.
54. Buenrostro,J.D., Giresi,P.G., Zaba,L.C., Chang,H.Y. and Greenleaf,W.J. (2013) Transposition of native chromatin for fast and sensitive epigenomic profiling of open chromatin, DNA-binding proteins and nucleosome position. *Nat. Methods*, **10**, 1213–1218.
55. Zhang,Y., Liu,T., Meyer,C.A., Eeckhoute,J., Johnson,D.S., Bernstein,B.E., Nusbaum,C., Myers,R.M., Brown,M., Li,W. *et al.* (2008) Model-based analysis of ChIP-Seq (MACS). *Genome Biol.*, **9**, R137.
56. Shin,H., Liu,T., Manrai,A.K. and Liu,X.S. (2009) CEAS: cis-regulatory element annotation system. *Bioinformatics*, **25**, 2605–2606.
57. Gel,B., Diez-Villanueva,A., Serra,E., Buschbeck,M., Peinado,M.A. and Malinverni,R. (2016) regioneR: an R/Bioconductor package for

the association analysis of genomic regions based on permutation tests. *Bioinformatics*, **32**, 289–291.
58. Chawla-Sarkar,M., Lindner,D.J., Liu,Y.F., Williams,B.R., Sen,G.C., Silverman,R.H. and Borden,E.C. (2003) Apoptosis and interferons: role of interferon-stimulated genes as mediators of apoptosis. *Apoptosis*, **8**, 237–249.
59. Thyrell,L., Erickson,S., Zhivotovsky,B., Pokrovskaja,K., Sangfelt,O., Castro,J., Einhorn,S. and Grander,D. (2002) Mechanisms of Interferon-alpha induced apoptosis in malignant cells. *Oncogene*, **21**, 1251–1262.
60. Chiappinelli,K.B., Strissel,P.L., Desrichard,A., Li,H., Henke,C., Akman,B., Hein,A., Rote,N.S., Cope,L.M., Snyder,A. *et al.* (2015) Inhibiting DNA methylation causes an interferon response in cancer via dsRNA including edogenous Retroviruses. *Cell*, **162**, 974–986.
61. Roulois,D., Loo Yau,H., Singhania,R., Wang,Y., Danesh,A., Shen,S.Y., Han,H., Liang,G., Jones,P.A., Pugh,T.J. *et al.* (2015) DNA-demethylating agents target colorectal cancer cells by inducing viral mimicry by endogenous transcripts. *Cell*, **162**, 961–973.
62. Leonova,K.I., Brodsky,L., Lipchick,B., Pal,M., Novototskaya,L., Chenchik,A.A., Sen,G.C., Komarova,E.A. and Gudkov,A.V. (2013) p53 cooperates with DNA methylation and a suicidal interferon response to maintain epigenetic silencing of repeats and noncoding RNAs. *Proc. Natl. Acad. Sci. U.S.A.*, **110**, E89–E98.
63. Kadota,S. and Nagata,K. (2014) Silencing of IFN-stimulated gene transcription is regulated by histone H1 and its chaperone TAF-I. *Nucleic Acids Res.*, **42**, 7642–7653.
64. Perez-Lluch,S., Blanco,E., Tilgner,H., Curado,J., Ruiz-Romero,M., Corominas,M. and Guigo,R. (2015) Absence of canonical marks of active chromatin in developmentally regulated genes. *Nat. Genet.*, **47**, 1158–1167.
65. Moerdyk-Schauwecker,M., Shah,N.R., Murphy,A.M., Hastie,E., Mukherjee,P. and Grdzelishvili,V.Z. (2013) Resistance of pancreatic cancer cells to oncolytic vesicular stomatitis virus: role of type I interferon signaling. *Virology*, **436**, 221–234.
66. Monsurro,V., Beghelli,S., Wang,R., Barbi,S., Coin,S., Di Pasquale,G., Bersani,S., Castellucci,M., Sorio,C., Eleuteri,S. *et al.* (2010) Anti-viral state segregates two molecular phenotypes of pancreatic adenocarcinoma: potential relevance for adenoviral gene therapy. *J. Transl. Med.*, **8**, 10.
67. Trojer,P., Zhang,J., Yonezawa,M., Schmidt,A., Zheng,H., Jenuwein,T. and Reinberg,D. (2009) Dynamic histone H1 isotype 4 methylation and demethylation by histone lysine methyltransferase G9a/KMT1C and the Jumonji domain-containing JMJD2/KDM4 proteins. *J. Biol. Chem.*, **284**, 8395–8405.
68. Trojer,P., Li,G., Sims,R.J. 3rd, Vaquero,A., Kalakonda,N., Boccuni,P., Lee,D., Erdjument-Bromage,H., Tempst,P., Nimer,S.D. *et al.* (2007) L3MBTL1, a histone-methylation-dependent chromatin lock. *Cell*, **129**, 915–928.
69. Kim,K., Choi,J., Heo,K., Kim,H., Levens,D., Kohno,K., Johnson,E.M., Brock,H.W. and An,W. (2008) Isolation and characterization of a novel H1.2 complex that acts as a repressor of p53-mediated transcription.*J. Biol. Chem.*, **283**,9113–9126.
70. Shen,Y.J., Le Bert,N., Chitre,A.A., Koo,C.X., Nga,X.H., Ho,S.S., Khatoo,M., Tan,N.Y., Ishii,K.J. and Gasser,S. (2015) Genome-derived cytosolic DNA mediates type I interferon-dependent rejection of B cell lymphoma cells. *Cell Rep.*, **11**, 460–473.
71. Rigby,R.E., Webb,L.M., Mackenzie,K.J., Li,Y., Leitch,A., Reijns,M.A., Lundie,R.J., Revuelta,A., Davidson,D.J., Diebold,S. *et al.* (2014) RNA:DNA hybrids are a novel molecular pattern sensed by TLR9. *EMBO J.*, **33**, 542–558.